Efficient extraction of past seawater Pb and Nd isotope signatures from Southern Ocean sediments

H. Huang[1]*, M. Gutjahr[1], G. Kuhn[2], Ed C. Hathorne[1], and A. Eisenhauer[1]

[1]GEOMAR Helmholtz Centre for Ocean Research Kiel, Kiel, Germany.

[2]Alfred-Wegener-Institut Helmholtz-Zentrum für Polar- und Meeresforschung, Bremerhaven, Germany.

Corresponding author: Huang Huang (huanghuang@mail.sysu.edu.cn)

*Current addresses: School of Marine Sciences, Sun Yat-Sen University, Zhuhai, China

Key Points:

- 10-seconds reductive leaching is capable of reliably extracting seawater Pb and Nd isotope signals from Southern Ocean sediments
- Natural porewater Pb isotopic compositions are analyzed for the first time in front of the Antarctic Filchner-Rønne Ice Shelf
- Presentation of first regional authigenic Pb and Nd isotopic signatures from 70 coretop sediments in the Atlantic sector of Southern Ocean

Abstract

Radiogenic lead (Pb) and neodymium (Nd) isotope compositions extracted from authigenic phases in marine sediments are sensitive tracers to reconstruct past ocean circulation and water mass mixing. Chemical reductive leaching of hydrogenetic ferromanganese oxyhydroxides from bulk sediments is the most practical way to recover past seawater Pb and Nd isotope signatures in the Southern Ocean, due to the scarcity of alternative archives. However, the leached signal could be compromised if substantial quantities of Pb and Nd were released from non-hydrogenetic sediment fractions during chemical extraction. Here we developed a very short 10-seconds leaching method to extract reliable seawater Pb and Nd isotope signals from sediments in the Atlantic sector of Southern Ocean. The effect of a previously recommended $MgCl_2$ prewash, the role of chelate ligands in the leaching solution and length of leaching time were investigated. The results show that 10 seconds exposure time of sediments to reductive leaching extracted sufficient and more reliable hydrogenetic Pb and Nd compared with the commonly used 30-minute leaching approaches. The robustness of our improved leaching method was validated via direct comparison of Pb and Nd isotope signatures with actual seawater, porewater and corresponding sediment leachates from three stations in front of the Antarctic Filchner-Rønne Ice Shelf. Our findings suggest that in contrast previously studied sites on the West Antarctic continental shelf, the southern Weddell Sea shelf is not a location of pronounced benthic Nd fluxes to the water column.

Plain Language Summary

Individual water masses in the modern ocean can often be identified by the isotopic signature of dissolved trace metals Pb and Nd which supplied from surrounding continents. By analyzing the past seawater Pb and Nd isotope ratios preserved in the sedimentary archives, we can understand how the ocean circulation changed. In the Southern Ocean, seawater Pb and Nd archives are very scarce. Thus, chemically extracting Pb and Nd from the seawater-derived ferromanganese oxyhydroxides within deep marine sediments becomes the most practical way to recover past seawater signal. However, Southern Ocean sediments commonly contain substantial Antarctic continental fine sediment, which easily partially dissolve during extraction, thereby releasing Pb and Nd, which did not originate from past ambient seawater. Here we established an efficient extraction method to obtain reliable past Southern Ocean seawater signatures. In addition, via analysis of regional seawater-derived Pb and Nd isotopic signatures from 70 surface sediments

in the Atlantic sector of Southern Ocean, we found that the sediments far away from Antarctica and volcanically active regions are generally credible to preserve unaltered seawater Pb and Nd isotope signals, which strongly supports the unique possibility of tracing past water mass sourcing in the Southern Ocean with our analytical approach.

1 Introduction

Radiogenic Pb and Nd isotope compositions have been successfully applied as sensitive and powerful palaeoceanographic proxies for the reconstruction of past circulation changes and water mass mixing for decades (Burton et al., 1997; Christensen et al., 1997; Frank, 2002; Foster & Vance, 2006; Huang et al., 2020). The radiogenic isotopes ^{206}Pb, ^{207}Pb and ^{208}Pb are produced by the decay of ^{238}U ($T_{1/2}$ = 4.47 Ga), ^{235}U ($T_{1/2}$ = 707 Ma) and ^{232}Th ($T_{1/2}$ = 14 Ga), while the radiogenic isotope ^{143}Nd is also produced by a very slow α-decay of ^{147}Sm ($T_{1/2}$ = 106 Ga). Because of these long half-lifes, crustal radiogenic/primordial isotopes ratios, i.e. $^{206}Pb/^{204}Pb$ and $^{143}Nd/^{144}Nd$ (commonly expressed in $\varepsilon_{Nd}=[(^{143}Nd/^{144}Nd)/0.512638–1]\times10^4$), are constant on relatively short Cenozoic timescales unless crustal reservoirs were mixed. Dissolved Pb and Nd in the oceans are mainly supplied by continental runoff, so Pb and Nd isotope signatures of the water masses are determined by the average regional crustal compositions of weathered continental crust (Frank, 2002; Goldstein & Hemming, 2003). Substantial quantities of dissolved Nd are also delivered to the oceans by sediment-bottom water exchange along continental margins (Lacan & Jeandel, 2005; Lacan et al., 2012) or oceanic islands (Rempfer et al., 2011; Stichel et al., 2012a; Pearce et al., 2013) . However, to date such a mechanism has not been reported for seawater Pb. This is (i) because of difficulties in acquiring reliable seawater Pb concentration data, and (ii) because Pb released from continental margin sediments is very likely efficiently re-adsorbed within sedimentary porewaters due to its high particle-reactivity. The average oceanic Nd residence time between 600 and 2000 years (Tachikawa et al., 1999; Tachikawa et al., 2003) allows ε_{Nd} to serve as a quasi-conservative water mass tracer away from ocean margins. In contrast to Nd, Pb has a much shorter residence time (50-200 years) (Schaule & Patterson, 1981; Cochran et al., 1990; Henderson & Maier-Reimer, 2002), allowing it to track local and generally rather proximal weathering inputs (Gutjahr et al., 2009; Kurzweil et al., 2010; Crocket et al., 2012; Crocket et al., 2013).

Various archives have been successfully employed to recover seawater Pb and Nd isotope signals in the past, such as fossil fish teeth/debris, fossil foraminifera, Fe-Mn crusts or nodules, sedimentary ferromanganese (Fe-Mn) oxyhydroxides and cold-water corals. In very early studies, extracting past seawater Pb and Nd isotope signals were mainly conducted using Fe-Mn crusts (Abouchami et al., 1997; Burton et al., 1997; Frank & O'Nions, 1998; O'Nions et al., 1998; Reynolds et al., 1999; Frank et al., 2002; van de Flierdt et al., 2004). However, due to its slow growth rate, Fe-Mn crusts are not suitable for generating records of (sub-) millennial resolution. Fossil fish teeth (Staudigel et al., 1985; Martin & Scher, 2004) and fossil foraminifera (Vance & Burton, 1999; Klevenz et al., 2008; Roberts et al., 2010) in marine sediments are both reliable archives for (sub-) millennial resolution seawater Nd isotope studies. However, fossil fish debris was found not to be suitable for Pb isotopic reconstructions (Basak et al., 2011). In addition, fossil foraminifera and fish debris are often not available in sufficient quantities for a hydrogenetic Nd isotope reconstruction of high precision and desired temporal resolution, especially in deep Southern Ocean sediments which are often carbonate-free. Cold-water corals represent a good alternative because their age can be well constrained. Nevertheless, only recently cold-water corals were shown to be a robust archive both for extracting seawater derived Pb (Lee et al., 2014; Lee et al., 2017; Wilson et al., 2017) and Nd (van de Flierdt et al., 2004; van de Flierdt et al., 2006; Colin et al., 2010; Wilson et al., 2014; Struve et al., 2017). However, fossil cold-water corals are usually not found in situ in abyssal water depths below the aragonite or calcite compensation depths. Furthermore, the extraction of coral-hosted Nd or Pb is tedious and multi-millennial continuous temporal coverage is often not achievable. Past seawater Pb and Nd isotope reconstructions generated via reductive leaching of sedimentary Fe-Mn oxyhydroxides in bulk sediments has also been established as a robust procedure in various deep marine settings (Gutjahr et al., 2007; Blaser et al., 2016). Since Southern Ocean sediments usually do not contain sufficient biogenic components, reductive leaching is so far the only practical option to extract deep sea Pb and Nd isotope signal in deep marine high latitude settings, which has also been successfully applied in carbonate-free Arctic sediments to obtain reliable bottom water Pb and Nd signal (Haley et al., 2008; Chen et al., 2012).

The previously reported reductive leaching methods for extracting authigenic Pb and Nd isotope signatures from marine sediments are slightly different from each other so some issues need to be addressed before the establishment of a refined extraction method for authigenic Fe-

Mn oxyhydroxide-sourced Pb and Nd. The first is whether it is necessary to pre-wash a sediment sample with $MgCl_2$ solution. The $MgCl_2$ pre-wash was proposed to remove potentially present contaminating phases prior to reductive Fe-Mn oxyhydroxide leaching. This technique was introduced decades ago (Tessier et al., 1979) and especially used for leaching sedimentary seawater-derived Pb (Gutjahr et al., 2007; Gutjahr et al., 2009). However, no study has as yet assessed the necessity of carrying out a $MgCl_2$ pre-wash from an isotopic perspective. Secondly, chelate ligands, like EDTA, were used in reductive leaching to prevent re-adsorption of released authigenically sourced trace metals (Gutjahr et al., 2007; Chen et al., 2012; Blaser et al., 2016),

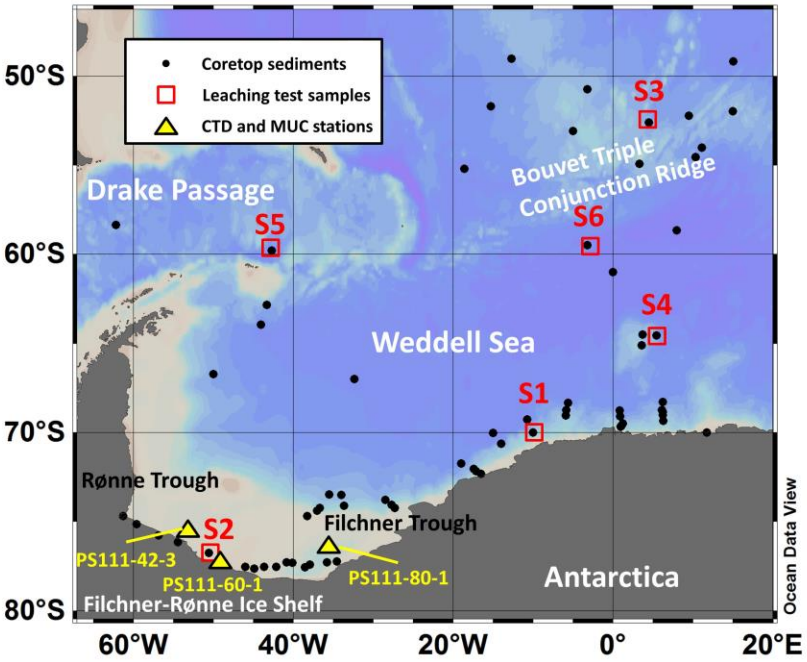

Figure 1. The locations of sample sites used in this study.

but many other studies did not add chelate ligands to their leaching reagents (Haley et al., 2008; Basak et al., 2011; Wilson et al., 2013; Du et al., 2016). The benefit of adding EDTA is to prevent re-adsorption via complexation of dissolved authigenic Pb (Gutjahr et al., 2007), yet whether adding ligands into the leaching solution may introduce contamination or cause undesired isotopic fractionation is as yet untested. In more recent studies, 30 minutes exposure time of sediments to chemical reagents was usually recommended as a suitable leaching time, without prior chemical carbonate removal (Wilson et al., 2013; Blaser et al., 2016; Du et al., 2016). Since shorter leaching time should dissolve less material from the non-hydrogenetic fraction, a very short contact time,

i.e. 10 seconds, should theoretically extract even purer hydrogenetic Pb and Nd isotope signal than 30 minutes leaching, especially for Southern Ocean sediments which commonly contain substantial quantities of only physically weathered continental detritus that is particularly susceptible for unwanted Rare Earth Element (REE) release during chemical extraction (Middelburg et al., 1988; Diekmann & Kuhn, 1999; Michels et al., 2002; Diekmann et al., 2003; Yusoff et al., 2013).

In this study, we investigated the effects of $MgCl_2$ pre-wash, presence or absence of chelate ligands and leaching time on extracted authigenic Nd and Pb isotope compositions in the Atlantic sector of Southern Ocean in order to optimise the leaching method. Since the ability that chemical extraction of sedimentary Fe-Mn oxyhydroxides can extract seawater Pb and Nd isotope signals is debated, we also analysed Pb and Nd isotopic compositions in seawater, porewater and leachates at three sampling stations in the front of Filchner-Rønne Ice Shelf in the southernmost accessible Weddell Sea area. The suggestion that sediment-sourced Nd is a dominant source for the global oceanic Nd budget (Tachikawa et al., 2003; Arsouze et al., 2009; Rempfer et al., 2011) is revisited for the southern Weddell Sea. We also generated Pb and Nd isotopic maps via analysis of 70 coretop sediment samples in the Atlantic sector of the Southern Ocean for a better understanding of the interaction between sediments and seawater in different geologic settings. These maps also allow identification of most suitable sediment core sites for palaeoceanographic studies.

2 Materials and Methods

2.1 Sample sites

The locations of seawater, porewater and sediment samples used in this study are shown in Figure 1. 70 coretop sediment samples were collected from the Alfred-Wegener-Institut (AWI) Core Repository in Bremerhaven (Germany) for leaching tests and regional mapping of sedimentary seawater-derived Nd and Pb isotopic compositions in the Atlantic sector of the Southern Ocean. Seawater samples for Pb and Nd isotope analyses were taken from three stations in front of the Filchner-Rønne Ice Shelf using Niskin bottles mounted onto a CTD-rosette during expedition

PS111 from January to March 2018 onboard RV Polarstern. Porewater and sediment samples were also retrieved at these three stations by multicore (MUC) sampling during the same cruise.

2.2 Leaching experiments

Although chemical reductive leaching has been applied to extract trace metals from marine Fe-Mn oxyhydroxides since the 1960s (Chester & Hughes, 1967), it is still under development to date. One major concern is that the leaching solution applied in the procedure inevitably dissolves both hydrogenetic fractions and non-hydrogenetic sediment components, such as continental detritus and volcanic ash, potentially contaminating the seawater-derived signal. There are two effective ways to minimize contamination: 1) using weak/diluted leaching solution and 2) short leaching time (Gutjahr et al., 2007; Chen et al., 2012; Wilson et al., 2013; Blaser et al., 2016). A smaller solution/solid ratio was also suggested to be an option to reduce contaminations (Wilson et al., 2013). In principal, the leaching reaction consumes chemicals, like hydroxylamine hydrochloride, in the leaching solution and a lower solution/solid ratio therefore result in a less aggressive leaching solution. Based on these two principals, a revised leaching procedure has been recently presented for the gentle extraction of a porewater Nd isotopic signature from bulk sediments in the Atlantic Ocean (Blaser et al., 2016). In the following, we refined this method to extract both seawater-derived Pb and Nd from Southern Ocean sediments. Furthermore, we investigated (i) the effect of the $MgCl_2$ pre-wash which was proposed to remove potentially present exchangeable contaminations (Tessier et al., 1979; Gutjahr et al., 2007) and (ii) the effect of chelate ligand used to prevent readsorption.

Six coretop sediment samples, named from S1 to S6 (Table S1), were selected for sequential leaching tests from different locations in the Atlantic sector of the Southern Ocean (Figure 1). The NOD-A-1 powder, a pure Fe-Mn oxyhydroxide nodule standard provided by the USGS, was used as a reference material. The published leaching procedure (Blaser et al., 2016) described below was used as the analytical protocol to be modified:

Conventional leaching: Approximately 0.5 g of wet bulk sediment or 0.05 g reference material was weighed in prior to chemical extraction. The weighed samples were agitated in the 15 mL leaching solution for 10 seconds on a vortex shaker to suspend the sediment and then in a regular shaker for 30 minutes. After centrifugation, 6 mL of the leachate was pipetted out for concentration

and isotope analysis. The leaching solution contained 0.005 M hydroxylamine hydrochloride (HH), 1.5 % acetic acid and 0.001 M EDTA buffered to pH~4 with suprapure NaOH (corresponding to a final molarity of ~0.033 M NaOH) in acid-cleaned polypropylene 50 mL centrifuge tubes. The buffering solution NaOH could also be replaced with suprapure ammonia (cf. Blaser et al. 2019), yet we did not employ this reagent here.

Following the conventional leaching procedure, a series of control leaching experiments were carried out on separate set of samples (S1 to S7) as followed:

1) Effect of $MgCl_2$ pre-wash: before conventional leaching, samples were mixed with 20 mL 1 M $MgCl_2$ solution for 1 hour in a shaker. After centrifugation at 2500 rpm and decanting of the supernatant, the samples were washed four times with 35 mL MilliQ water, followed by centrifugation for five minutes at 3000 rpm and decanting of the supernatant.

2)Effect of chelate ligands: Two different leaching solutions were modified from conventional leach solution: one used diethylenetriaminepentaacetic acid (DTPA) to replace EDTA and another without chelating ligands inside. Samples were processed with the conventional 30-minutes leaching method with these two different leaching solutions.

3) 10-seconds leaching: samples were only exposed to leaching solution for 10 *seconds* on the vortexing shaker without further 30 min leaching in the regular shaker.

4)Sequential leaching: after 30 min conventional leaching, samples were centrifuged, the supernatant extracted, new leaching solution added, and samples were leached again with 15 mL new leaching solution for 60 min. Following centrifugation, removal of the supernatant, addition of new leaching solution the samples were leached for another 180 min and this last leachate fraction was subsequently collected too.

2.3 Seawater Pb and Nd

The best way to validate a leaching method is to directly compare the actual seawater isotope signal with corresponding leachate isotopic compositions. Unfortunately, the modern-day natural seawater Pb is entirely contaminated by anthropogenic sources but a very recent study showed that seawater very close to Antarctica is still relatively unaffected containing about 95% natural Pb

(Ndungu et al., 2016). This suggests that seawater Pb in remote Antarctic ocean basins protected under sea ice should be more natural than anywhere else. Therefore, we sampled seawater at around 76° S on the Antarctic shelf in front of Filchner-Rønne Ice Shelf for Pb and Nd isotope analysis (Figure 1) where seawater is covered by sea ice during most of the year.

Shelf seawater samples used in this study were collected from different depths in the water column using Niskin bottles mounted on a stainless steel CTD rosette and multicore (MUC) for shelf bottom water. In order to distinguish seawater sampled by CTD and MUC, we denote these as CTD seawater and MUC bottom water, respectively. While seawater sampling for Nd isotopic analyses are commonly undertaken using this seawater sampling approach, for seawater Pb collection usually trace metal-clean approaches are necessary (Rijkenberg et al., 2015). Since such a sampling device was not available during PS111, potential Pb contamination is a concern. The Pb contamination issue is discussed later in section 4.1.

The seawater samples were filtered through a 0.2/0.8 µm Acropak® filter and then acidified to pH ~2 using double distilled concentrated nitric acid. From each depth, ~10-20 L seawater was collected in acid-cleaned 20 L LDPE-collapsible cubitainers for Nd isotopes analysis, 1 L seawater was collected in acid-cleaned 1 L PE bottle for Pb isotope analysis and 250 mL seawater sample was collected in acid-cleaned 250 mL PE bottles for Pb and Nd concentration measurements. Besides the 20 L samples for Nd isotope analysis, all other samples were only filtered and acidified on board and further processed in the GEOMAR Kiel (Germany) clean laboratory facilities.

The ~10-20 L seawater samples for Nd isotopic analysis were further processed on board by adding purified dissolved Fe–chloride solution. After 6 hours equilibration time, ammonia solution (25%, Mercksuprapur®) was added to raise the pH to 7.5-8.5 in order to co-precipitate dissolved Nd with iron oxyhydroxides. After settling of the precipitates, most of the supernatant was discarded and the residue was transferred into 1 L acid-cleaned PE-bottles for transport to the home laboratory.

After transport to the clean room facilities at GEOMAR Kiel, the iron oxyhydroxide precipitates were transferred in acid-cleaned 50 mL centrifuge tubes and centrifuged for 10 minutes at 4000 rpm. Subsequently samples were rinsed at least two times with Milli-Q water followed by centrifugation to wash out major ions (Ca, Mg, K etc.). The precipitates were dissolved in 2 mL 6 M HCl and transferred into 30 ml Teflon vials to dry down on the hotplate. Subsequently, 2 mL

aqua regia (HNO_3: HCl = 1:4) was added, refluxed for 24 hours and afterwards dried down. Then 2 mL of 6 M HCl was added and dried down again to transfer back to Cl-form. Before column purification, the excess amount of Fe is separated from the sample via Fe back extraction. For this step, each dried sample was re-dissolved in 4 ml of 6M HCl and mixed with a suitable amount (about 3 mL) cleaned di-ethyl ether (Stichel et al., 2012b). About 90% of dissolved iron can be extracted into the organic solution phase and discarded. This Fe-extraction procedure was repeated twice or more often until the sample solutions became pale yellow. After evaporation, the seawater samples were re-fluxed in 2 ml 6M HCl and dried down again before the subsequent cation exchange purification step.

For the extraction of Pb and Nd from CTD seawater Pb and MUC bottom water, 5 mL of concentrated ammonia solution (25%, Mercksuprapur®) is added into 1 L acidified seawater samples to raise the pH to 10. After 2 days of reaction time, white $Mg(OH)_2$ precipitates slowly form. The supernant was then discarded and the white residue dissolved in 6 mL 2M HBr/0.1M HF solution for further ion chromatographic Pb and Nd purification.

2.4 MUC sediment and porewater

All operations for porewater sampling from MUC sediments were undertaken in a glove bag under oxygen-free conditions in an argon gas atmosphere. The acid-cleaned centrifuge tubes and sample bottles were also flushed with argon gas before use. After extraction of overlying seawater via siphoning, the MUC sampling tube was transferred into the glove bag and MUC sediment was sampled in 2 cm increments on a Teflon sampling stand. Each 2 cm sub-sample was transferred in a 50 mL centrifuge tube. The porewater was separated from sediment by centrifugation at 4000 rpm for 60 minutes. Consequently, the porewater was filtered through a pre-cleaned 0.2 µm Supor®filter and acidified to pH~2. About 10-20 mL porewater samples were recovered from each depth from one sample tube. The remaining sediment samples were kept for reductive leaching experiments. All samples were transported back home for further chemical purification and isotope measurements at GEOMAR Kiel.

Dissolved Pb contained in sediment porewaters was directly dried down for Pb column purification without any additional treatment in order to minimize potential blank contributions. Authigenic

Pb in the remaining MUC sediment samples was extracted using the 10-seconds leaching method (detailed in section 2.2) before purification by ion chromatography.

2.5 Authigenic Pb and Nd isotopic coretop sediment mapping

A total of 70 coretop sediment samples were processed using the 10-seconds leaching method described in section 2.2 for the generation of authigenic Pb and Nd isotopic maps of the Atlantic sector of the Southern Ocean. The Pb and Nd aliquots were purified by ion chromatography.

2.6 Ion chromatography

The Pb cuts in the porewater and leachates were purified by ion chromatography on miniaturized columns containing ~80 µL AG1-X8 resin (Lugmair & Galer, 1992).The MUC bottom water and

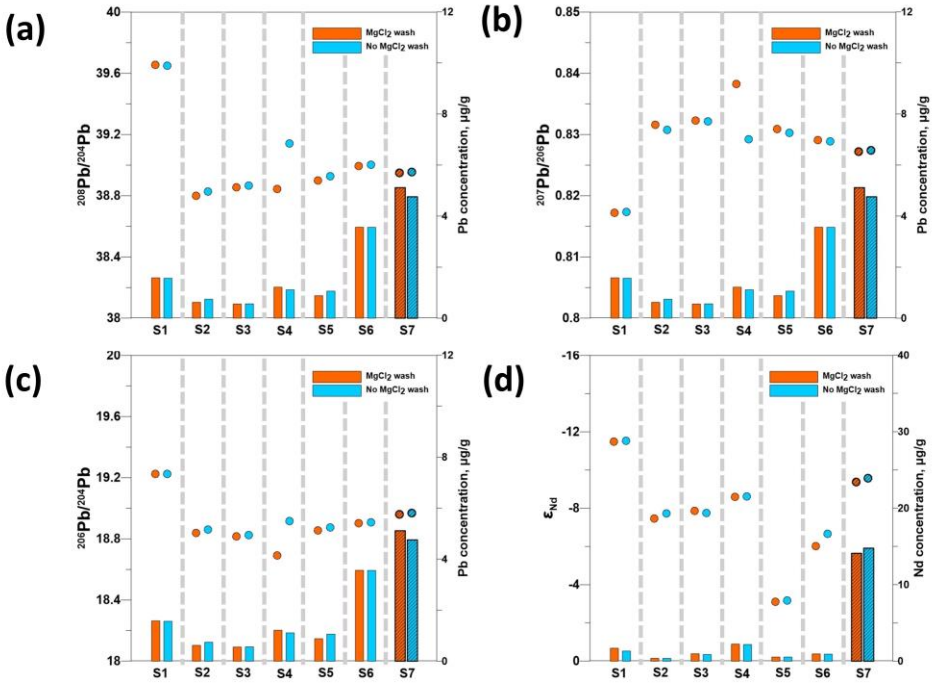

Figure 2 Effect of $MgCl_2$ pre-wash. Round dots indicate isotopic compositions and bar charts indicate recovery concentrations in the leachates. (a) $^{208}Pb/^{204}Pb$ and Pb concentration. (b) $^{207}Pb/^{206}Pb$ and Pb concentration. (c) $^{206}Pb/^{204}Pb$ and Pb concentration. (d) ε_{Nd} and Nd concentration. The results conducted by USGS NOD-A-1 standard (S7) are highlighted with stippled bar charts.

CTD seawater Pb cuts, which were pre-concentrated using the $Mg(OH)_2$ co-precipitation method, can form substantial quantities of silicate gel and clog the column during normal Pb chromatography. In order to dissolve the silicate gel, 6 mL 2 M HBr/0.1 M HF was added to the

$Mg(OH)_2$ precipitate from each 1L seawater sample. The protocol (Table S2) used to purify Pb is modified from an earlier study (Paul et al., 2015a). After Pb purification, the remaining REE cuts were separated by cation exchange chromatography using 50W-X8 resin followed by separation of Nd from the other REE using LN-Spec resin (Cohen et al., 1988).

2.7 Mass spectrometry

Element concentrations were measured with an Agilent 7500-CE Quadrupole ICP-MS at GEOMAR Kiel. Two different standard calibrations were employed to cover samples of high and low trace element concentrations with reproducibility strongly dependent on the respective element. All concentration results were normalized to the initially used sample weight (in µg/gram of wet bulk sediment weighed in).

Seawater Pb and Nd concentration measurements were conducted on a 7 mL sample loop using an online pre-concentration technique (OP) ICP-MS at GEOMAR employing an automated "SeaFast" system (Elemental Scientific Inc.) coupled to a Thermo Scientific Element XR. The Pb and Nd concentration was analyzed with the same established method used for REE concentration measurements (Hathorne et al., 2012). During measurements, reference seawater BATS, CAB and MF-20 solutions were used to assess the reproducibility and accuracy of the data.

Pb and Nd isotope measurements were performed on a Thermo Scientific Neptune Plus MC-ICP-MS at GEOMAR, Kiel. Mass bias correction during Pb isotope measurements was done externally using the Tl-doping technique (Belshaw et al., 1998; Süfke et al., 2019) with added NIST997 Tl standard solution. Given that Tl and Pb fractionate slightly differently during ionization, $^{205}Tl/^{203}Tl$ were determined on a session-by-session basis so that NBS981 Pb isotope compositions matched published compositions (Thirlwall, 2002; Baker et al., 2004; Süfke et al., 2019) . Total Pb procedural blanks in leachates and seawater samples were below 50 pg (n=30) and are hence negligible. The total Pb procedural blanks in porewater were below 2 pg (n=2) and the sample were between 50 and 100 pg, so the blank Pb contaminations were lower than 4%. The

reproducibility of the secondary standard USGS NOD-A-1 is listed in Table S3. As shown in the table, all measured standard Pb isotopic ratios are within the error of published compositions.

Instrumental mass fractionation during Nd isotopic analyses was corrected by normalizing the measured ratio of $^{143}Nd/^{144}Nd$ to $^{146}Nd/^{144}Nd = 0.7219$ and $^{142}Nd/^{144}Nd = 1.141876$ using the mass bias correction procedure of Vance and Thirlwall (2002). The measured Nd isotope ratios were

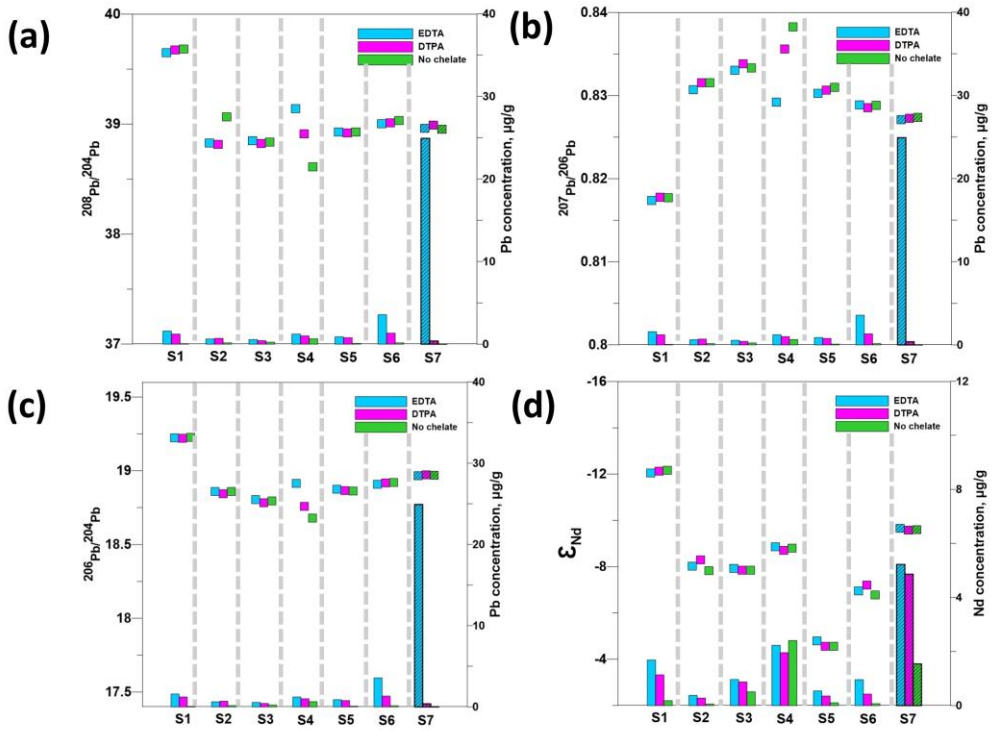

Figure 3 Effect of chelating ligands. Square dots illustrate Pb isotopic compositions or ε_{Nd} in the leachates; Bar charts show Pb or Nd concentration values in the leachates. (a) $^{208}Pb/^{204}Pb$ and Pb concentration. (b) $^{207}Pb/^{206}Pb$ and Pb concentration. (c) $^{206}Pb/^{204}Pb$ and Pb concentration. (d) ε_{Nd} and Nd concentration. The results conducted by USGS NOD-A-1 standard (S7) are distinguished with stippled bar charts.

normalized to the published $^{143}Nd/^{144}Nd$ value of 0.512115 for JNdi-1 (Tanaka et al., 2000). Total procedural blanks for Nd are below 30 pg and hence negligible (n=20). Secondary standard solution NIST 3135a was run with the samples to check the external reproducibility.

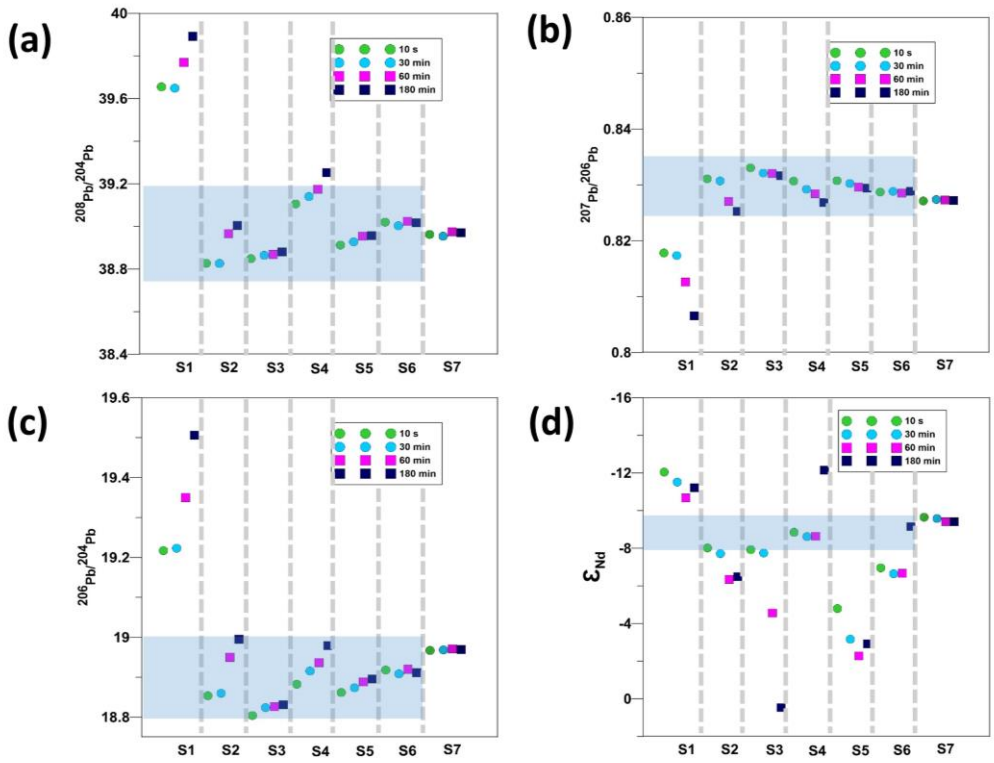

Figure 4 Effect of leaching time on Pb and Nd isotopic compositions. (a) $^{208}Pb/^{204}Pb$, (b) $^{207}Pb/^{206}Pb$, (c) $^{206}Pb/^{204}Pb$ and (d) ε_{Nd}. The round dots show results of 10-s leaching and 30-min conventional leaching, obtained separately with fresh samples. The square dots show leaching results carried out by mixing 30-min leaching residues with renewed leaching solution for 60 min, and again with renewed leaching solution for 180 min. The blue shades indicate the range of expected SO seawater Pb and Nd isotope signatures (Abouchami & Goldstein, 1995; Stichel et al., 2012b).

The secondary standard NIST 3135a reproduced within 0.2 ε_{Nd} for a 50 ppb solution (n=169, 2 SD), and 1.25 ε_{Nd} for a 2 ppb concentration (n=5, 2 SD; see Table S4).

3 Results

3.1 Effect of $MgCl_2$ pre-wash

The Pb isotopic compositions of $MgCl_2$ pre-washed samples were all either identical within error or less radiogenic (lower) in $^{206}Pb/^{204}Pb$ and $^{208}Pb/^{204}Pb$ compared to the samples processed without $MgCl_2$ pre-wash (Figure 2a and c). Only sample (S1) was not affected by $MgCl_2$ pre-wash (Figures 3). In contrast to the obtained Pb isotopic results, Pb concentrations recovered by these

two approaches were almost identical. On the other hand, both ε_{Nd} and Nd concentrations extracted from all samples are within error both with or without preceding $MgCl_2$ pre-wash (Figure 2d).

3.2 Effect of chelate ligand

Leaching solutions containing EDTA and DTPA had a much higher Pb and Nd recovery rate than solutions without ligands (Figure 3). This result clearly shows that the lack of chelating ligands in the leaching solution leads to pronounced Pb and Nd re-adsorption during chemical extraction. Between the two tested ligands, EDTA shows a stronger complexation ability both towards Nd and Pb than DTPA. Although ligands have a strong influence on the Pb and Nd recovery rate, all ε_{Nd} values and most $^{206}Pb/^{204}Pb$, $^{208}Pb/^{204}Pb$ and $^{207}Pb/^{206}Pb$ ratios produced from these samples are identical within error, indicating that the addition of ligands neither introduces contamination nor causes isotopic fractionation. Only $^{208}Pb/^{204}Pb$ of S2 and all displayed Pb isotopic ratios in S4 leachates in Figure 3 produced divergent results as a function of chelating reagent used.

3.3 Effect of leaching time

A wide range of leaching times, from 10 seconds to 180 minutes, was investigated for all samples. The Pb and Nd isotopic compositions sequentially leached out from the USGS NOD-A-1 standard are obviously invariant, because it is a largely homogeneous Fe-Mn oxyhydroxide-based material. $^{206}Pb/^{204}Pb$ and $^{208}Pb/^{204}Pb$ in the sediment leachates were generally increasing and $^{207}Pb/^{206}Pb$ were decreasing with extended leaching time. Sediments from sites S1, S2 and S4 which were sampled close to the Antarctic continent showed the most pronounced offsets with increasing leaching time. In contrast, sequential leaching had only little or no impact on Pb isotope signatures of the samples, S3, S5 and S6 that were derived from deep open ocean locations (Figures 1, 4a, b and c). Similar to Pb isotopic compositions, ε_{Nd} values in sediment leachates also shifted towards more radiogenic (higher) values from 10 seconds to 60 minutes leaching but reversed to less radiogenic (low) values or increased to very high $\varepsilon_{Nd}>0$ of S3 at 180 minutes, indicating leaching

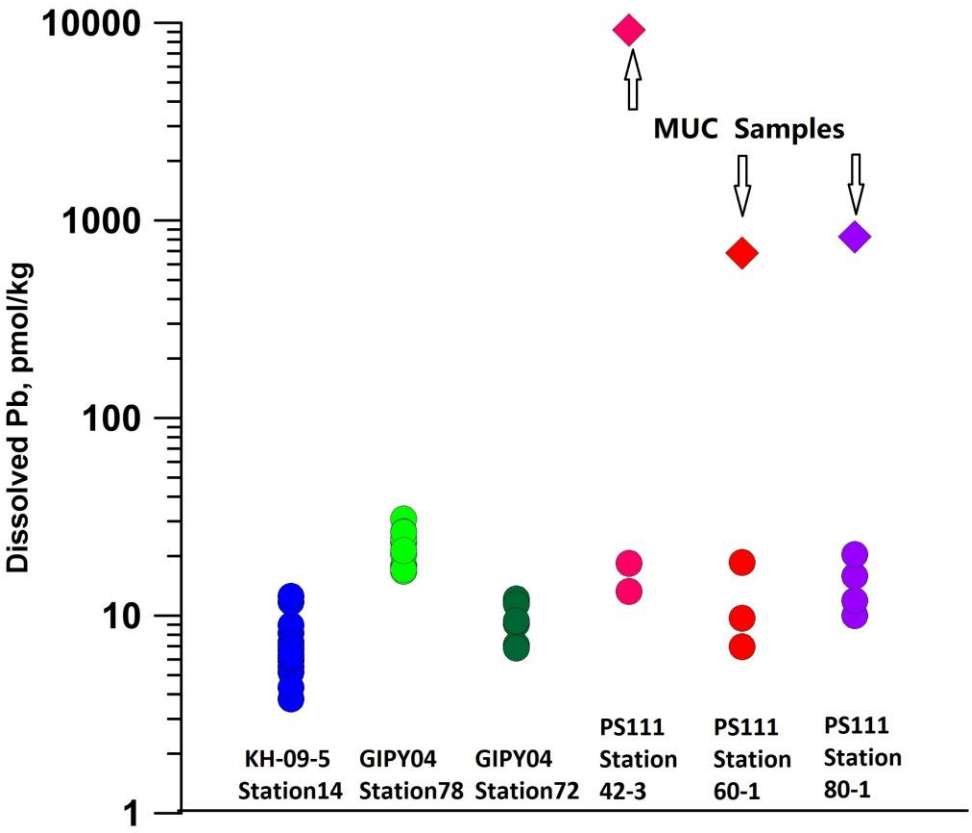

Figure 5 Comparison of seawater Pb concentrations collected from cruise PS111 and two close GEOTRACES stations (KH-09-5 and GIPY04). The seawater samples collected by CTD are marked by round dots and recovered by MUC are showed as diamonds. The seawater Pb concentration data of KH-09-5 (Lee et al., 2015) and GIPY04 (Schlitzer et al., 2018) were taken from the GEOTRACES database.

342

343 at 180 minutes targeted different sediment fractions with distinct ε_{Nd} compositions (Figure 4d).

344 3.4 Filchner-Rønne shelf seawater Pb and Nd

345 As evident from Figure 5, seawater Pb concentrations collected by CTD at these three stations
346 from cruise PS111 match the seawater Pb concentration range sampled in previous studies using
347 trace metal clean devices at nearby GEOTRACES stations, while Pb concentrations collected by
348 MUC are extremely high indicating an anthropogenic contamination. Generally, the seawater Pb
349 and Nd concentrations along the Filchner-Rønne Ice Shelf (Figure 6a and b) either scatter around
350 mean low concentrations or increase with increasing water depth, while two Pb concentrations at
351 150 and 100 meter water depths of PS111-42-3 and PS111-60-1 are elevated. Correspondingly,
352 the $^{206}Pb/^{204}Pb$ ratios of these two samples are very unradiogenic. The Nd isotope compositions of
353 Filchner-Rønne shelf seawater showed remarkably little deviation from an average ε_{Nd} =-

9.25±0.35 (2 SD), which agree with published Weddell Sea Deep and Bottom Water ε_{Nd} signatures further north between -8.4 and -9.6 (Stichel et al., 2012b). The seawater $^{206}Pb/^{204}Pb$ ratios of CTD station PS111-80-1 increase from 18.18 to 18.72 with increasing water sampling depth. This station also shows a quasi-linear increase of Pb concentrations with water depth from 10 pmol/kg in 20 meter water depth to 20 pmol/kg at 930 meter (i.e., 5 meters above the seafloor).

3.5 Pb and Nd isotopic compositions in leachates and MUC porewater

Due to insufficient quantities of available Nd in extracted porewater (below 0.2 ng at each depth), the Nd isotopic compositions in the porewaters were not analyzed. Porewater Pb concentrations are also depleted but Pb isotopic compositions from some depths could still be determined. We only compared $^{208}Pb/^{206}Pb$ in the porewater because ^{208}Pb and ^{206}Pb are the two most abundant Pb isotopes in nature, hence providing the best possible precision among all Pb isotopic ratios. In Figure 7, the MUC bottom water $^{208}Pb/^{206}Pb$ at three stations are identical ($^{208}Pb/^{206}Pb$=2.12) and very distinct from seawater $^{208}Pb/^{206}Pb$ in the water column above. We also noticed more than 10 times higher recovered Pb concentrations in MUC bottom water than in CTD seawater (Figure 5). The suspect MUC seawater Pb isotopic signature is evidently overprinted by Pb contamination sourced from the MUC sampler itself because Pb bricks are used as a weight mounted on top of the MUC sampling tubes. The $^{208}Pb/^{206}Pb$ in the upper few centimeters within the sediment porewater also shifted towards the distinct Pb contamination signature seen in MUC bottom water, suggesting that Pb derived from the MUC weights also invaded the top centimeters of the sediment porefluids. However, the porewater $^{208}Pb/^{206}Pb$ below about 8 cm were resolvably not affected by this downcore Pb diffusion and agree with $^{208}Pb/^{206}Pb$ values in sediment leachates extracted using the 10-seconds leaching method. The CTD sampled shelf bottom water $^{208}Pb/^{206}Pb$ at our three sampled stations is consistently in the range of 2.07, which is only slightly offset from the coretop leachate ($^{208}Pb/^{206}Pb$ =2.05 to 2.06). Since the seawater sampling setup was not trace metal clean and recovered porewater Pb concentrations were very low, improved approaches in the future should lead to a better match between bottom water compositions and coretop sediment leachates.

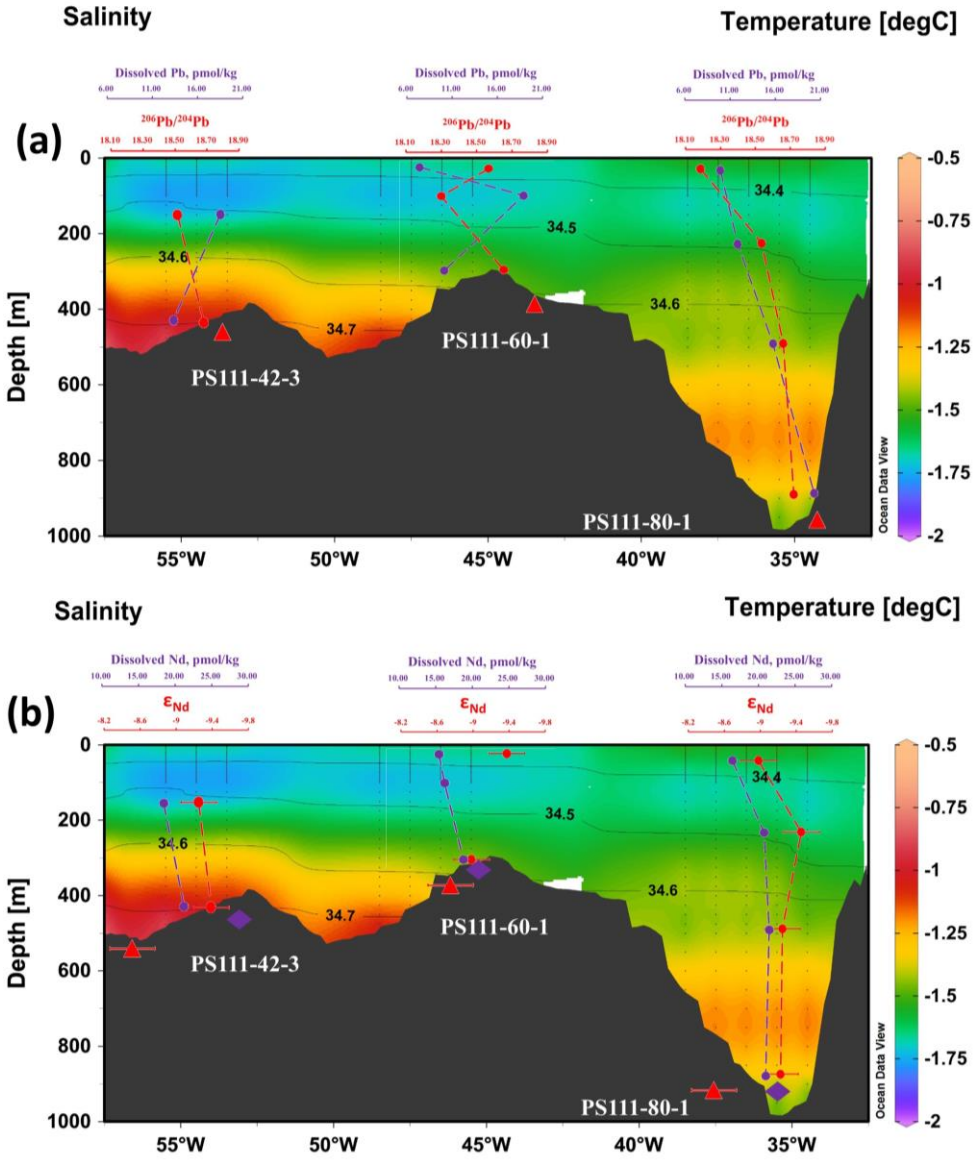

Figure 6 Concentrations and isotopic compositions of seawater Pb and Nd with hydrological context in front of Filchner-Rønne Ice Shelf (sample sites indicated in Fig. 1). (a) Pb dataset; (b) Nd dataset. Round dots indicate seawater data. The purple diamonds show Nd concentrations in MUC bottom water. The red triangles indicate authigenic isotopic compositions extracted from coretop sediments at the first centimeter core depth. Color-mapped seawater temperature, with salinity contours overlain, as drawn from the 2009 World Ocean Atlas (Zweng et al., 2013).

These results demonstrate that authigenic Pb extracted from Weddell Sea shelf sediments using the improved reductive leaching approach reflect the porewater Pb isotope signal derived from bottom water.

The Nd concentrations in MUC bottom water samples, ranging from 21 to 28 pmol/kg (Figure 6b), are slightly higher than the bottom water sampled by CTD several meters above, but only 3 liters

of filtered seawater were recovered from each MUC station. The very low quantities of Nd recovered from MUC seawater resulted in highly expanded measurement uncertainties. The average MUC bottom water ε_{Nd} value of -8.9±2.4 from these three stations, however, is identical to bottom seawater at all three stations. Similar to Pb, the average ε_{Nd} extracted via reductive leaching from the top 10 cm of sediment are consistent in all three cores, ranging from -8.4 to -8.8 but are slightly offset from overlying CTD seawater and MUC seawater ε_{Nd} signature (Figure 7) on the order of 0.3 to 0.9 ε_{Nd}.

3.6 Authigenic Pb and Nd isotopic variability in the Atlantic sector of the Southern Ocean

Figure 8 shows three different Pb isotope signature regimes on the map: $^{206}Pb/^{204}Pb<18.5$, $^{206}Pb/^{204}Pb>19.0$ along the East Antarctic continental margin and other areas with an average Weddell Sea $^{206}Pb/^{204}Pb$ of about 18.8 (Abouchami & Goldstein, 1995). Authigenic ε_{Nd} coretop compositions also allow defining three areas which are slightly different from areas defined via $^{206}Pb/^{204}Pb$ (Figure 8b). Extracted ε_{Nd} found to the east of the Drake Passage and in the northeast at the Bovet Triple Conjunction are more radiogenic than ambient seawater with $\varepsilon_{Nd}>-6$. Coretop sediments near the East Antarctic continent have the most unradiogenic ε_{Nd} ranging from -10.3 to -12.5, also deviating from regional bottom water compositions. The rest of the ε_{Nd} values extracted from coretop sediments agree with published seawater ε_{Nd} signatures (Stichel et al., 2012b).

4 Discussion

4.1 Seawater Pb and Nd on the Filchner-Rønne shelf

The seawater Pb samples collected for this study were sampled by a standard CTD approach, which is not trace metal clean, so the samples were potentially contaminated to some extent. One indicator as to whether the sampled seawater Pb is contaminated is the dissolved Pb concentration, where high Pb concentration values in the sample is a sign of contamination. Reported seawater Pb concentrations in the Atlantic sector of Southern Ocean from previous GEOTRACES cruises GA10 and GIPY04 are lower than 23 pmol/kg (Schlosser et al., 2019) and 31 pmol/kg (Schlitzer et al., 2018), respectively. Sampled Pb in all our seawater samples collected by CTD are below 21 pmol/kg (Figure 5), with minimum concentrations as low as 7 pmol/kg, indicating no significant contaminations, while the concentrations of the contaminated Pb samples collected via

the separate MUC approach are on the order of 600 pmol/kg or higher. The seawater Pb isotopic composition is another important indicator for Pb contamination. Anthropogenic Pb usually has characteristically unradiogenic Pb isotopic signatures (Bollhöfer & Rosman, 2000; Lee et al., 2015). As shown in Figure 6a, the shelf bottom water $^{206}Pb/^{204}Pb$ ratios at these three stations are very consistent at around 18.7 which agree with recently reported Antarctic Bottom Water (AABW) $^{206}Pb/^{204}Pb$ ratios of 18.68 and 18.78 in the Indian sector of Southern Ocean (Lee et al., 2015), suggesting that the Pb contamination from our standard CTD sampling process is negligible.

However, the authigenic $^{206}Pb/^{204}Pb$ ratio extracted from the coretop sediments right below the CTD stations are more radiogenic, ranging from 18.80 to 18.88, than the bottom water Pb isotope signal (Figure 6a). The slightly less radiogenic bottom water Pb isotope signal

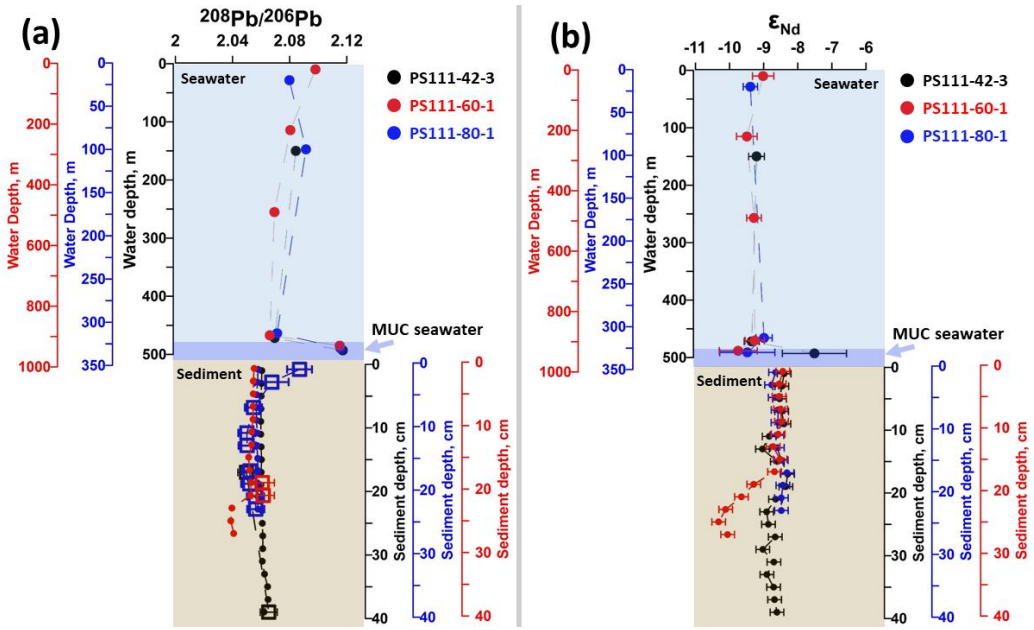

Figure 7 Pb and Nd isotopic compositions in sampled shelf seawater, MUC-sampled bottom water, extracted porewater and leachates at three stations in front of Filchner-Rønne Ice Shelf. (a) $^{208}Pb/^{206}Pb$ and (b) ε_{Nd}. The round dots in the seawater and sediment boxes indicate seawater and leachate isotopic compositions. The empty square dots indicate porewater $^{208}Pb/^{206}Pb$ ratios.

is deemed to reflect minor anthropogenic contributions to the natural Pb isotope signature, either introduced during sampling or being controlled by minor ambient anthropogenic Pb presence in the sampling area. One possible source of dissolved anthropogenic Pb onto Filchner-Rønne shelf is Modified Warm Deep Water (MWDW) invading from the northern Weddell Sea which contains inherited North Atlantic Deep Water (NADW) contributions. An influence of MWDW inflow to

the Filchner-Rønne shelf was also found in an earlier clay mineral assemblage study in the Weddell Sea (Ehrmann et al., 1992).Modern dissolved Pb in NADW is enriched in anthropogenic Pb in the South Atlantic (Schlosser et al., 2019). The MWDW is present on the Ronne side (western side in Figure 6a) of the Filchner-Rønne shelf at ~150 m water depth (Nicholls et al., 2003). Correspondingly, the dissolved Pb with elevated concentration and unradiogenic $^{206}Pb/^{204}Pb$ at depth between 150 and 100 m are observed at PS111-42-3 and PS111-60-1. Another possible entranceway of anthropogenic Pb is via atmospheric deposition in surface seawater. The $^{206}Pb/^{204}Pb$ ratio of surface seawater at PS111-60-1 and PS111-80-1 are all very low which can be supplied by unradiogenic anthropogenic Pb derived from dust (Bollhöfer & Rosman, 2000; 2002) as previously found in a nearby ice core (Planchon et al., 2003). Alternatively it could be released by ice rafted debris transported across this area, which also contained a very unradiogenic $^{206}Pb/^{204}Pb$ signature (Flowerdew et al., 2013). Dissolved anthropogenic Pb in the upper water column can shift the bottom water Pb isotope signal via vertical particle flux through the water column without direct water mass mixing (Wu et al., 2010), leading to

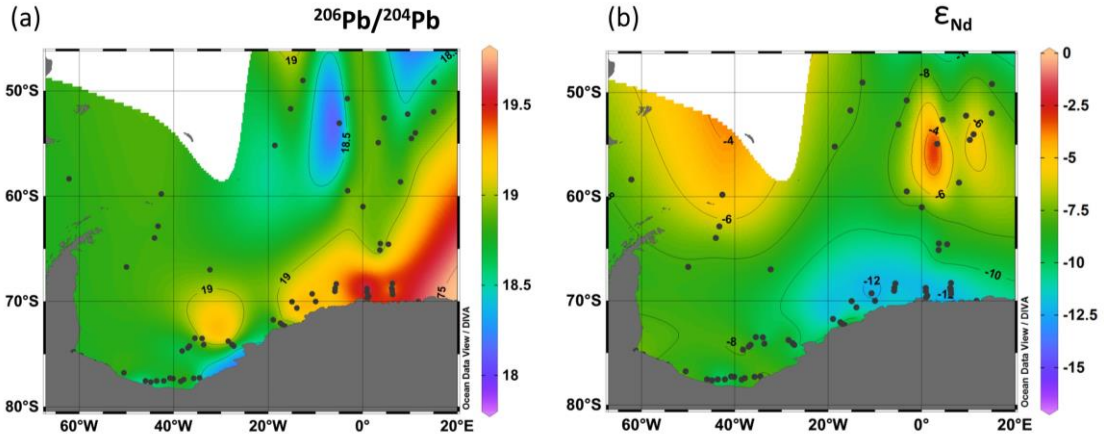

Figure 8 Authigenic $^{206}Pb/^{204}Pb$ and ε_{Nd} isotopic maps generated from coretop sediments in the Atlantic sector of the Southern Ocean. (a) $^{206}Pb/^{204}Pb$ and (b) ε_{Nd}.

the offset between preindustrial authigenic Pb signal in the coretop sediment and bottom water.

Anthropogenic Pb signals have previously been observed in authigenic Pb extracted from North Atlantic marine (Crocket et al., 2013) and Swiss Alpine lake sediments (Süfke et al., 2019). Here this anthropogenic signal seems to disappear at the sediment-bottom water interface in the three cores in front of Filchner-Rønne Ice Shelf since their authigenic Pb isotope signals are identical to the 20 cm of sediment below that clearly have an undisturbed natural composition (Figure 7a).

Very low sedimentation rates of Filchner-Rønne shelf sediment could explain this feature, where 1 cm of coretop sediment could cover several thousand years (Hillenbrand et al., 2014), the postindustrial layer, thus, might only present a rather small fraction at the topmost sediment surface which has insignificant contribution to the uppermost authigenic Pb isotope signal that represents the homogenized average composition of the top two centimeters.

The vertical and lateral distribution of Nd concentrations in the studied section (Figure 6b) is similar to the general pattern in the Weddell Sea (Stichel et al., 2012a). The surface seawater Nd concentrations at Filchner-Rønne shelf, between 14.1 and 18.3 pmol/kg, agree with the average surface dissolved Nd concentration of 18 pmol/kg in the northern Weddell Sea. The slightly higher Nd concentrations at depth are also in agreement with comparable water depth data in the open Weddell Sea, and can be explained by reversible particle scavenging (Siddall et al., 2008; Stichel et al., 2012b). The benthic flux was suggested to dominate seawater Nd isotope signatures near the continent in settings such as the eastern North Pacific (Abbott et al., 2015a; Abbott et al., 2015b) or deglacial deep Labrador Sea (Blaser et al., 2020), similar to our studied area. Strikingly, highly elevated bottom water Nd concentrations that were observed at various shelf locations in front of the West Antarctic Ice Sheet that were almost twice the concentration seen at similar water depths offshore (Carter et al., 2012; Rickli et al., 2014) are not found in the southernmost Weddell Sea (Figure 6b). This observation suggests absence of pronounced Nd boundary additions to the bottom water on the Filchner-Rønne shelf at the three core locations.

Neodymium in Weddell Sea sediments is distributed in two major pools: 1) authigenic Fe-Mn oxyhydroxides and 2) the terrigenous phase. The mobilization of Fe-Mn oxyhydroxide-bound Nd should be largely suppressed here because it takes place under reducing conditions (Haley et al., 2003).The bottom water on the Filchner-Rønne shelf, however, is one of the most oxygen-enriched water masses in the world (Orsi & Whitworth, 2005). As to the terrestrial detritus, if detrital Nd partially dissolved, it should first affect local porewater compositions, a process which is bound to be recorded by concomitantly forming authigenic Nd signatures, before such an elevated Nd flux was released to local bottom water. As shown in the Figure 6b, only the bottom water at PS111-60-1 shift towards the authigenic ε_{Nd} extracted in the coretop sediment. Therefore, a diffusive benthic Nd flux is probably not a major source of dissolved Nd on the Filchner-Rønne shelf. Substantial quantities of Weddell Sea AABW is initially formed on the Filchner-Rønne shelf, then

481 circulating in the Weddell Sea Gyre (Vernet et al., 2019) and partially laterally returning back as
482 part of MWDW (Nicholls et al., 2009). As a result, the ε_{Nd} signatures of water masses on the
483 Filchner-Rønne shelf is likely well-homogenized and isotopically very similar to Weddell Sea
484 Deep Water (i.e., the variety of AABW that is exported from the Weddell Sea) (Orsi & Whitworth,
485 2005; Stichel et al., 2012b).

486 4.2 Measures for reliable porewater Pb and Nd isotope extraction from Southern Ocean sediments

487 Most Pb isotope signals extracted from the samples pre-treated with $MgCl_2$ were shifted towards
488 less radiogenic Pb isotope compositions in $^{208}Pb/^{204}Pb$-$^{206}Pb/^{204}Pb$ space (Figure 9), with this
489 contribution likely being of anthropogenic origin. Because $MgCl_2$ solution is the only variable
490 factor in this experiment, the external Pb contamination was most likely sourced from the $MgCl_2$
491 solution itself. As shown in Figure 2 and Figure 9, samples with low authigenic Pb concentrations
492 (S2 to S5) are more affected due to relatively higher proportions of Pb contamination from $MgCl_2$
493 solution in the extracted aliquots. However, neither the most affected sample S4 featured the
494 lowest concentration nor did the least affected sample S1 yield the highest concentration. As a
495 result, the sample lithology should also play a role in the process as some samples may contain
496 organic matter, which can preferentially absorb more Pb (Strawn & Sparks, 2000). Interestingly,
497 we did not observe substantial changes in Pb concentration while the Pb isotopic composition
498 clearly was altered. The process might take place under a solution-particle exchange equilibrium
499 affecting only Pb isotope compositions but not concentrations, as seen in seawater (Wu et al.,
500 2010). Background Nd concentrations in inorganic chemicals are commonly much lower than
501 respective Pb contaminations, so neither Nd concentration nor isotopic compositions were altered
502 by $MgCl_2$ pre-wash, which is similar to what has been found before (Haley et al., 2008). Since we
503 found $MgCl_2$ to potentially introduce Pb contamination into the sample, while we conversely

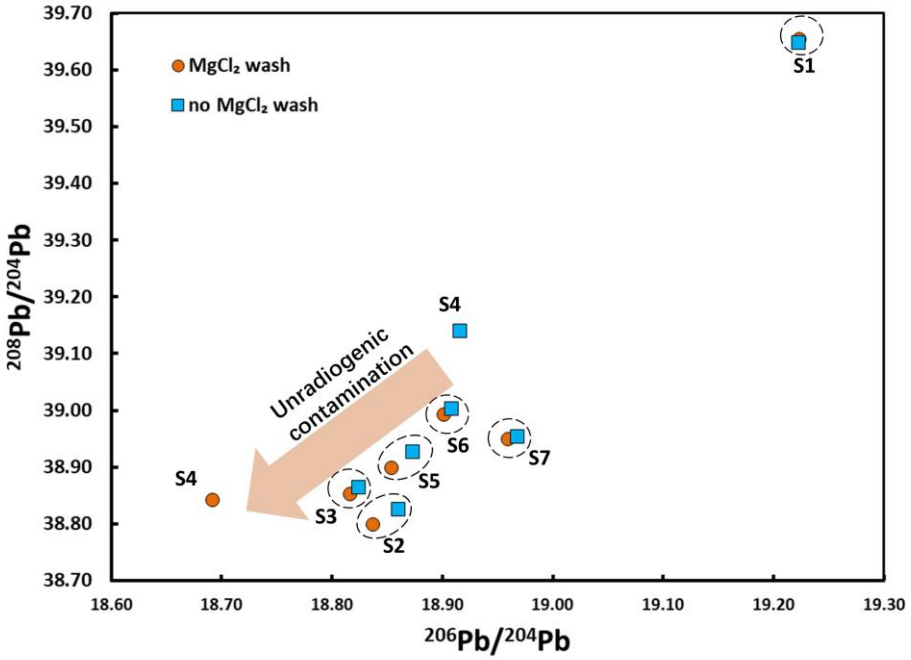

Figure 9 $MgCl_2$ pre-wash effects on Pb isotopic composition extracted from leaching test samples in $^{208}Pb/^{204}Pb$-$^{206}Pb/^{204}Pb$ spacing.

observed no significant improvement of extracted Nd signatures, we suggest avoiding the $MgCl_2$ pre-wash step preceding reductive leaching.

Previous leaching protocols that used EDTA required less than one gram of sediment (Gutjahr et al., 2007; Blaser et al., 2016) but an alternative approach without ligands suggested using sometimes more than 10 grams of sediment (Wilson et al., 2013). As shown in Figure 3, adding EDTA equally strongly prevents re-adsorption of Nd and we suggest using EDTA in the leaching solution in order to keep sediment usage at a minimum. We also demonstrated that it is safe to use EDTA because no significant contamination and isotopic fractionation was found in our experiments. The only exception is mainly S4 in which Pb isotopic compositions in the leachates were shifted when using different ligands but ε_{Nd} values remained identical. Re-adsorption of Pb is unlikely to cause such shifts in Pb isotopic composition since this offset was not observed in other samples when the re-adsorption effect was equally effective. One possible reason is that the sample was not perfectly homogenized. As shown in Figure 11, the leachate without ligands in S4 show lower Al/Pb and Al/Nd ratios than leachate with EDTA, while in the majority of the other samples the results are reversed. It clearly indicates that the portion of the S4 sample used for leaching without ligands contains materials that released substantial extra quantities of Pb and Nd

with altered Pb isotope signal but hydrogenetic Nd signature which could probably be fossil fish teeth (Basak et al., 2011). Although the reason for this effect is not entirely clear, leaching with EDTA still resulted in $^{206}Pb/^{204}Pb$ compositions within the seawater signature range and in

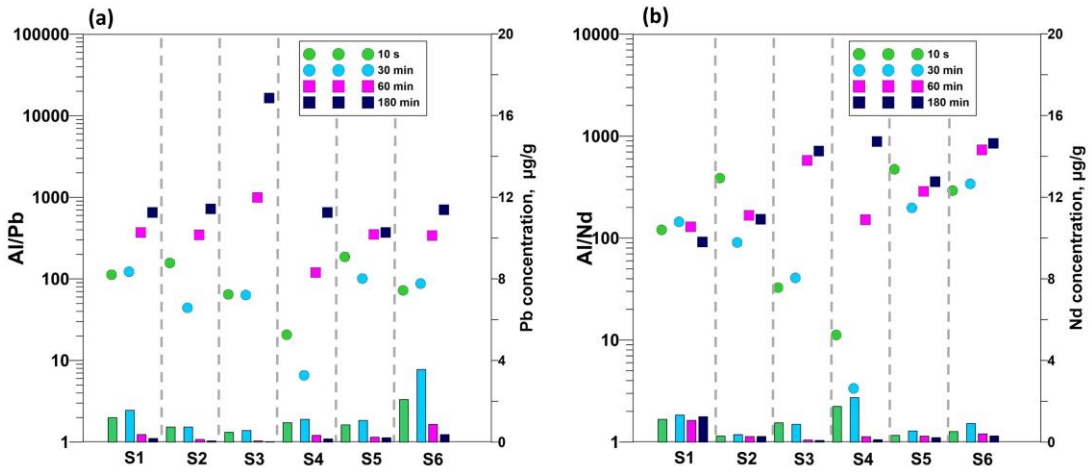

Figure 10. Variations of Al/Pb, Al/Nd, Pb and Nd concentrations of sediment samples during the sequential leaching. (a) Al/Pb and Pb concentration. (b) Al/Nd and Nd concentration. Green circle dots indicate Al/Pb or Al/Nd of 10-s leaching. Square dots indicate Al/Pb or Al/Nd of sequential leaching. Bar charts show extracted Pb and Nd concentrations.

agreement with neighboring coretop sediment sampling stations (Figure 8a) while $^{206}Pb/^{204}Pb$ are too low (<18.76) when using DTPA or no reductive the leaching solution without ligands.

One general observation from previous reductive leaching studies for Nd is that shorter leaching times appear to provide more reliable results by dissolving less non-authigenic sedimentary phases (Gutjahr et al., 2007; Gourlan et al., 2010; Wilson et al., 2013; Blaser et al., 2016). Compared with the 10-seconds leaching approach, both Pb and Nd isotope signals extracted via the recently recommended 30-minute leaching duration are always more radiogenic and closer to the subsequent one-hour sequential leaching signals which contained a higher proportion non-hydrogenetic Pb and Nd (Figure 4), indicating that a 10 second exposure to leaching acquired the purest hydrogenetic signals. Although the ε_{Nd} in S5 and S6 even for samples with the shortest exposure time are offset by Nd additions from regional volcanic substrate in the sediment (Latimer et al., 2006), 10 seconds leaching still led to ε_{Nd} values closer to actual seawater compositions (Figure 4d). A common reservation towards only leaching sediments for 10 seconds is that the Pb and Nd recovered may not be sufficient for isotope analysis. However, we found that the 10-

seconds vortexing leaching recovered more or less the same amount of Pb and Nd as extracted during 30 minutes of leaching (Figure 10a and b).

It has been found that Nd extracted from authigenic Fe-Mn oxyhydroxides via the reductive leaching method in many cases provides identical results to Nd extraction from sedimentary foraminifera, which in turn reflect the porewater origin of the Nd isotope signal (Blaser et al., 2016). The porewater Nd isotope signal is derived from overlying seawater and sometimes modified by benthic exchange processes with the detrital phase (Abbott et al., 2015a). We also observed that the ε_{Nd} values extracted using the 10-seconds leaching method from three MUC sediment cores provided compositions slightly offset from MUC and CTD seawater Nd isotope signature immediately above the sediment (Figure 7b) within 1 ε_{Nd}. The ε_{Nd} deviation between porewater and overlying seawater is likely caused by settle release of Nd from IRD and/or clays in the sediment because these three MUC sediments are all dominantly muddy with substantial quantities of IRD present inside. Previous studies showed that IRD (Blaser et al., 2019), poorly weathered material (Howe et al., 2016) and clays (Ohr et al., 1991) could both release Nd from the terrigenous fraction during early diagenesis.

Another important finding of this study is that the Pb isotope signal obtained via 10-seconds leaching of MUC sediments is identical to the porewater Pb isotope signal. Compositions are only slightly offset from bottom seawater Pb isotope signatures sampled via CTD (Figure 7a), although the latter may also be induced by the non-trace metal clean water sampling approach. Although it is generally assumed that the Pb isotope signature preserved in sedimentary authigenic Fe-Mn oxyhydroxides records a porewater signal, for the first time this assumption could be validated by actual corresponding porewater Pb isotope compositions.

4.3 Elemental ratios as proxies for non-hydrogenetic contamination

Elemental ratios in reductive Fe-Mn oxyhydroxide leachate solutions were previously used as proxies for monitoring non-hydrogenetic contamination: 1) REE patterns for the origin of Nd (Bayon et al., 2002; Martin et al., 2010); 2) Al/Pb and Al/Nd for non-hydrogenetic phases (Gutjahr et al., 2007). REE patterns were not investigated in this study because these were recently shown to be unreliable for the identification of contaminating phases (Blaser et al., 2016). Al/Pb and Al/Nd ratios were used to monitor dissolution of the detrital and potentially present volcanogenic

fraction, due to high Al/Pb and Al/Nd ratios in non-hydrogenetic phases and low ratios in hydrogenetic phases (Gutjahr et al., 2007). However, care should be taken to compare like with like. If the degree of re-adsorption affects or even dominates the concentration for highly particle reactive elements, the application of this proxy may be limited and the Al/Pb and Al/Nd ratios then only reflect the different re-adsorption behavior of Al, Pb and Nd. As shown during the tests constraining the efficiency of chelating ligands, the extracted Pb and Nd isotopic compositions were identical in individual samples (Figure 3) but the Al/Pb and Al/Nd (Figure 11) fluctuated dramatically, i.e. Al/Pb of S7 ranged from 10 to 10,000. Leaching without EDTA, in most cases, led to high Al/Pb and Al/Nd, indicating more Pb and Nd were re-adsorbed during reductive dissolution of the Fe-Mn oxyhydroxide phase.

When EDTA was used to prevent re-adsorption during leaching, Al/Pb and Al/Nd worked well in sequential leaching tests with exposure times from 30 min to 180 min (Figure 10a and b). For example, the Nd isotope signals in S5 and S6 were offset by volcanogenic contributions leading to high Al/Nd (cf. Blaser et al., 2016). Moreover, the ε_{Nd} values in 30 min sediment leachates (S2, S3 and S6) are consistent with seawater ε_{Nd} yielding Al/Nd lower than 100, which is similar to a threshold ratio for good quality Nd isotope data found in previous studies (Gutjahr et al., 2007; Blaser et al., 2016). However, the 10-seconds leaching method did not always result in lower Al/Pb

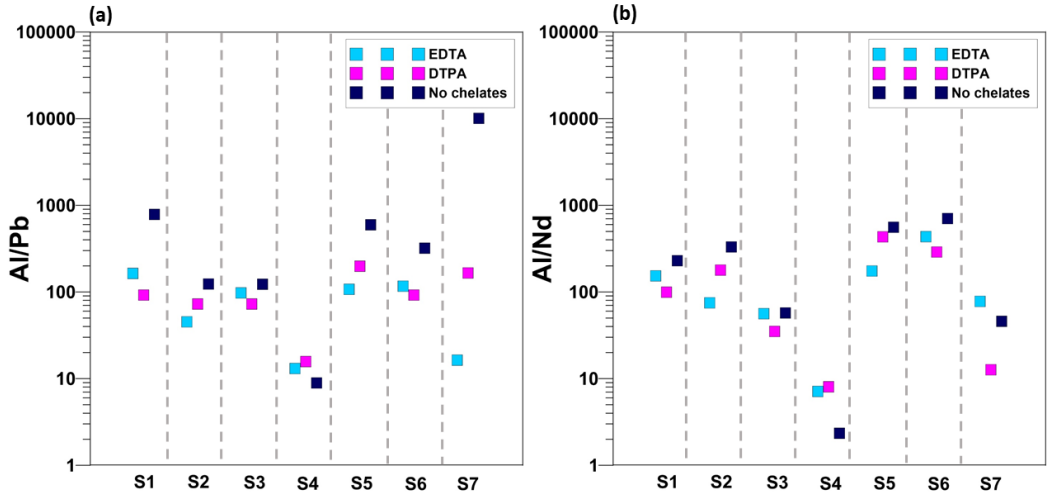

Figure 11. Variations of Al/Pb and Al/Nd of all samples using different ligands in the leaching solution. (a) Al/Pb. (b) Al/Nd.

and Al/Nd than 30 min leaching, although 10-seconds leaching extracted a purer hydrogenetic Pb and Nd portion from the bulk sediments as indicated by the respective isotopic compositions. More

specifically, we found, i.e. in S2, the amount of extracted Pb and Nd are similar during 10-second or 30-minute leaching, but the Al concentration extracted by 10-seconds leaching was much higher than by 30-minute leaching thus resulted in high Al/Pb and Al/Nd ratios using the 10-seconds leaching approach. Generally, Al^{3+} in the solution starts to precipitate at pH = 3.7 and almost quantitatively precipitates at pH = 4.7. The 30-minute leaching consumed more acetic acid than 10-second which leads to higher pH value in the solution, so the lowered Al concentration in the 30-minute leaching was likely caused by preferential Al precipitation due to the pH increase. These considerations reveal that the elemental behaviour during leaching can be complex so that the interpretation based on elemental concentrations and ratios should be made very carefully, even though in the large majority of cases in our experiments the low Al/Pb and Al/Nd ratio (<100) indicated reliable hydrogenetic Pb and Nd extraction.

4.4 Identifying sampling areas for SO-wide palaeocirculation reconstructions away from localized Antarctic depocenters

The Nd isotope composition extracted from bulk sediment can be altered by the partial dissolution of sedimentary components, such as volcanic ash (Elmore et al., 2011; Blaser et al., 2016), continental detrital phases (Pöppelmeier et al., 2018; Blaser et al., 2019) and pre-formed ferromanganese coatings (Bayon et al., 2004; Kraft et al., 2013; Pöppelmeier et al., 2018). As shown in Figure 8b, these unwanted Nd disturbances also exist at various sites in Southern Ocean sediments. However, the potential Pb interferences for reductive leaching are to date not as well investigated as for Nd. In this study, we generated corresponding $^{206}Pb/^{204}Pb$ and ε_{Nd} maps from coretop sediments to help identifying potential localized Pb disturbances in Southern Ocean sediments (Figure 8). Firstly, our data revealed that both $^{206}Pb/^{204}Pb$ (>19.0) and ε_{Nd} (from -10.3 to -12.5) extracted from coretop sediments near the East Antarctic continent are offset from nearby seawater ε_{Nd} and Pb isotope signatures reported from surface scrapings of Fe-Mn nodules (Abouchami & Goldstein, 1995). These could be caused by partially dissolving continental detritus or/and pre-formed ferromanganese coatings during leaching. Partial dissolution of detrital components in the sediment should lead to high Al/Pb and Al/Nd ratios in the leachates (Gutjahr et al., 2007; Blaser et al., 2016), but the Al/Pb and Al/Nd ratios of the 10-s S1 leachate (Figure 10) are low, indicating that our leaching approach did not significantly target the detrital fraction. Therefore, regionally or locally supplied continental Pb and Nd isotope signatures in pre-formed

Fe-Mn oxyhydroxides likely overprinted both extracted seawater-derived Pb and Nd from authigenic Fe-Mn oxyhydroxides in sediments near the Antarctic continental margin because reductive leaching inevitably dissolves both authigenic and pre-formed Fe-Mn oxyhydroxides (Bayon et al., 2004). The pre-formed Fe-Mn oxyhydroxides in the study area could for example be supplied by nearby ice streams (Rignot et al., 2011).

Secondly, the extracted ε_{Nd} from sediments located to the east of Drake Passage and in the Bouvet Triple Conjunction ridge display too radiogenic values compared with ambient deep water compositions due to Nd release from volcanic components within the sediments from nearby volcanic sources (Stichel et al., 2012ba). The elevated Al/Nd ratios in S5 and S6 (Figure 10b) also point towards contributions of volcanic material. Interestingly, Pb in S5 and S6 10-seconds leachates seems to be unaffected by volcanic contributions as we did not observe equally elevated Al/Pb in samples S5 and S6 (Figure 10a). Furthermore, $^{206}Pb/^{204}Pb$ extracted from sediments in the area enriched in volcanic materials area did not display compositions offset from expected seawater signals (Abouchami & Goldstein, 1995). Taken together, these observations suggest that the extraction of authigenic Pb may be less susceptible to analytically introduced artefacts than seen for authigenic Nd.

Although extracted Pb is apparently relatively robust against contamination by sedimentary volcanic material, anthropogenic Pb contributions supplied by dust can alter the natural seawater signal. Pb extracted from coretop sediments in the northeast of the research area closest to South Africa are extremely altered by anthropogenic Pb contamination (Figure 8). The lack of sea ice protection and relative proximity to the African continent could both result in the strong anthropogenic Pb footprint in these surface sediments, because winter sea ice does not extend that far north and Pb sourced from Africa was found in nearby water masses (Paul et al., 2015b). However, as shown in Figure 7a, anthropogenic Pb only penetrated the topmost few centimeters in the sediment. Thus, the extracted downcore Pb isotope signals in the lower parts should not be affected. Overall, the sediment core sites located in the green area in the open ocean (Figure 8) are recommended for downcore Pb and Nd isotope analysis for the purpose of ocean circulation

reconstructions because the extracted Pb and Nd isotope signals agree with open Southern Ocean seawater signatures.

In (near-)glacial settings Pb has been reported to be released incongruently resulting in more radiogenic Pb isotope signals during early chemical weathering stages (Erel et al., 2004) which has been successfully applied for monitoring deglacial continental weathering in both North Atlantic (Foster & Vance, 2006; Gutjahr et al., 2009; Kurzweil et al., 2010; Crocket et al., 2012) and Antarctica (Basak & Martin, 2013). The sequential leaching tests carried out on sediments very close to Antarctica (S1, S2 and S4 in Figure 4) under extended leaching conditions in fact represent a good simulation of temporal chemical weathering trends. More radiogenic Pb isotope signals were extracted from these sediments with increasing exposure time to reductive leaching. However, these weathering induced radiogenic Pb signals are efficiently diluted in the open ocean and deviated from the Fe-Mn nodule recorded seawater Pb signals (Figure 4). On the other hand, recent studies reported the absence of incongruent weathering effects on the Pb isotopic runoff signal both in experimental studies (Dausmann et al., 2019) and in a Holocene Alpine lake sediment record (Süfke et al., 2019). To what extent some or all of the marginal Antarctic authigenic Pb isotope signatures recorded incongruent supply of weathered Pb from inland Antarctica therefore requires further research.

5 Conclusions

We developed a fast 10-seconds leaching method to extract authigenic Pb and Nd isotope signatures from Southern Ocean sediments and validated this method by directly comparing the Pb and Nd isotope signal in sediment leachates with overlying seawater Nd and Pb isotopic signatures and corresponding Pb porewater compositions. Utilizing the 10-seconds leaching method established in this study, we screened coretop sediments in the Atlantic sector of Southern Ocean for their hydrogenetic Pb and Nd isotope distribution in order to identify suitable sediment core sites for future paleoceanographic reconstructions.

The use of a previously employed sedimentary pre-leaching cleaning technique using $MgCl_2$ was evaluated. Furthermore, the effect of using or omitting chelate ligands was assessed, and the optimal leaching time was determined. Our data show that the $MgCl_2$ wash is not necessary and, on the other hand, may potentially contaminate the authigenic Pb isotope signature in sedimentary samples. Experiments to constrain the effect of chelating ligands were carried out by

two commonly used ligands, EDTA and DTPA. Adding the chelating ligands during leaching was confirmed to be very important for leaching. When the leaching process was carried out without ligands, both Pb and Nd were substantially re-adsorbed back to the sediment. Between these two ligands, EDTA most efficiently prevented re-adsorption both for Pb and Nd, while no mass fractionation or contamination was observed. Moreover, the sequential leaching test indicated that the very short 10-seconds leaching extracted the purest hydrogenetic Pb and Nd signatures in all tested sediment samples and recovered sufficient quantities of Pb and Nd for isotope analysis. Therefore, we recommend using the 10-seconds leaching method in combination with EDTA to extract hydrogenetic Pb and Nd in Southern Ocean sediments.

The analysis of Pb and Nd isotope seawater signatures and porewater Pb isotopic compositions demonstrated that the extracted hydrogenetic Pb and Nd by 10-seconds leaching in our settings reflect the porewater isotope signals which may, however, in places be slightly offset from ambient seawater signal due to early diagenetic porewater processes.

The previously suggested leaching quality assessment proxies, Al/Nd and Al/Pb, also provide a critical insight regarding the nature of the extracted phase for Southern Ocean sediments when EDTA is present during leaching. The low Al/Nd and Al/Pb ratios (<100) in our experiments reflect the predominant extraction of a Fe–Mn oxyhydroxide phase but the high Al/Nd and Al/Pb ratios did not necessarily reflect tapping of the detrital phase since slow pH increase during longer leaching unavoidably induces Al precipitation and complex re-adsorption reactions.

The 10-seconds leaching is not omnipotent for extracting hydrogenetic Pb and Nd in all oceanographic settings due to potential presence of a benthic flux and pre-formed continentally derived ferromanganese oxyhydroxides. Therefore, we generated authigenic Pb and Nd isotopic maps for the Atlantic sector of Southern Ocean to avoid areas of altered sediment and localize suitable sites for generating authigenic Pb and Nd isotope reconstructions for the late Pleistocene. As a general guide, suitable core sites should be further away from the Antarctic continental margin to prevent input of significant pre-formed ferromanganese oxyhydroxides. In the case of authigenic Nd, the sediments should contain no or only minute quantities of volcanic material as suggested previously. The Pleistocene Nd and Pb isotopic evolution of Southern Ocean water masses such

as AABW and Circumpolar Deep Water are largely unresolved to date and our approach has the potential to provide reliable new key information at high temporal resolution in the coming years.

Acknowledgments, Samples, and Data

Sediment material for this study was obtained from the AWI core repository in Bremerhaven. We thank Jutta Heinze, Tyler Goepfert, Ana Kolevica, Bettina Domeyer and Michael Seebeck for technical support. We also thank the chief scientist Michael Schröder, Captain Stefan Schwarze and the crew of Polarstern for their contribution. Markus Janout, Hartmut Hellmer, Claudia Hanfland and Andreas Wisotzki helped with CTD seawater sampling, while Maria-Elena Vorrath and Hannes Grobe are thanked for their help during MUC sampling. Florian Scholz is acknowledged for advice and introduction on the MUC porewater sampling technique using glove bags. H. Huang acknowledges the China Scholarship Council (CSC) for providing financial support to his overseas study. Metadata and other results from the sediment cores, porewater and seawater are available within the Pangaea data base (DOI in preparation).

References

Abbott, A. N., B. A. Haley, and J. McManus (2015a), Bottoms up: Sedimentary control of the deep North Pacific Ocean's εNd signature, *Geology*, *43*(11), 1035-1035.

Abbott, A. N., B. A. Haley, J. McManus, and C. E. Reimers (2015b), The sedimentary flux of dissolved rare earth elements to the ocean, *Geochimica Et Cosmochimica Acta*, *154*, 186-200.

Abouchami, W., and S. L. Goldstein (1995), A lead isotopic study of circum-antarctic manganese nodules, *Geochimica et Cosmochimica Acta*, *59*(9), 1809-1820.

Abouchami, W., S. L. Goldstein, S. J. G. Gazer, A. Eisenhauer, and A. Mangini (1997), Secular changes of lead and neodymium in central Pacific seawater recorded by a Fe-Mn crust, *Geochimica et Cosmochimica Acta*, *61*(18), 3957-3974.

Arsouze, T., J. C. Dutay, F. Lacan, and C. Jeandel (2009), Reconstructing the Nd oceanic cycle using a coupled dynamical – biogeochemical model, *Biogeosciences*, *6*(12), 2829-2846.

728 Baker, J., D. Peate, T. Waight, and C. Meyzen (2004), Pb isotopic analysis of standards and
729 samples using a 207Pb–204Pb double spike and thallium to correct for mass bias with a double-
730 focusing MC-ICP-MS, *Chemical Geology*, *211*(3), 275-303.

731 Basak, C., and E. E. Martin (2013), Antarctic weathering and carbonate compensation at the
732 Eocene–Oligocene transition, *Nature Geoscience*, *6*, 121.

733 Basak, C., E. E. Martin, and G. D. Kamenov (2011), Seawater Pb isotopes extracted from Cenozoic
734 marine sediments, *Chemical Geology*, *286*(3), 94-108.

735 Bayon, G., C. R. German, K. W. Burton, R. W. Nesbitt, and N. Rogers (2004), Sedimentary Fe–
736 Mn oxyhydroxides as paleoceanographic archives and the role of aeolian flux in regulating oceanic
737 dissolved REE, *Earth and Planetary Science Letters*, *224*(3), 477-492.

738 Bayon, G., C. R. German, R. M. Boella, J. A. Milton, R. N. Taylor, and R. W. Nesbitt (2002), An
739 improved method for extracting marine sediment fractions and its application to Sr and Nd isotopic
740 analysis, *Chemical Geology*, *187*(3), 179-199.

741 Belshaw, N. S., P. A. Freedman, R. K. O'Nions, M. Frank, and Y. Guo (1998), A new variable
742 dispersion double-focusing plasma mass spectrometer with performance illustrated for Pb isotopes,
743 *International Journal of Mass Spectrometry*, *181*(1), 51-58.

744 Blaser, P., J. Lippold, M. Gutjahr, N. Frank, J. M. Link, and M. Frank (2016), Extracting
745 foraminiferal seawater Nd isotope signatures from bulk deep sea sediment by chemical leaching,
746 *Chemical Geology*, *439*, 189-204.

747 Blaser, P., M. Gutjahr, F. Pöppelmeier, M. Frank, S. Kaboth-Bahr, and J. Lippold (2020), Labrador
748 Sea bottom water provenance and REE exchange during the past 35,000 years, *Earth and*
749 *Planetary Science Letters*, *542*, 116299.

750 Blaser, P., et al. (2019), The resilience and sensitivity of Northeast Atlantic deep water εNd to
751 overprinting by detrital fluxes over the past 30,000 years, *Geochimica et Cosmochimica Acta*, *245*,
752 79-97.

753 Bollhöfer, A., and K. J. R. Rosman (2000), Isotopic source signatures for atmospheric lead: the
754 Southern Hemisphere, *Geochimica et Cosmochimica Acta*, *64*(19), 3251-3262.

755 Bollhöfer, A., and K. J. R. Rosman (2002), The temporal stability in lead isotopic signatures at
756 selected sites in the Southern and Northern Hemispheres, *Geochimica et Cosmochimica Acta*,
757 *66*(8), 1375-1386.

758 Burton, K. W., H.-F. Ling, and R. K. O'Nions (1997), Closure of the Central American Isthmus
759 and its effect on deep-water formation in the North Atlantic, *Nature*, *386*(6623), 382-385.

760 Carter, P., D. Vance, C. D. Hillenbrand, J. A. Smith, and D. R. Shoosmith (2012), The neodymium
761 isotopic composition of waters masses in the eastern Pacific sector of the Southern Ocean,
762 *Geochimica et Cosmochimica Acta*, *79*, 41-59.

763 Chen, T.-Y., M. Frank, B. A. Haley, M. Gutjahr, and R. F. Spielhagen (2012), Variations of North
764 Atlantic inflow to the central Arctic Ocean over the last 14 million years inferred from hafnium
765 and neodymium isotopes, *Earth and Planetary Science Letters*, *353-354*, 82-92.

766 Chester, R., and M. J. Hughes (1967), A chemical technique for the separation of ferro-manganese
767 minerals, carbonate minerals and adsorbed trace elements from pelagic sediments, *Chemical*
768 *Geology*, *2*, 249-262.

769 Christensen, J. N., A. N. Halliday, L. V. Godfrey, J. R. Hein, and D. K. Rea (1997), Climate and
770 Ocean Dynamics and the Lead Isotopic Records in Pacific Ferromanganese Crusts, *Science*,
771 *277*(5328), 913-918.

772 Cochran, J. K., T. McKibbin-Vaughan, M. M. Dornblaser, D. Hirschberg, H. D. Livingston, and
773 K. O. Buesseler (1990), 210Pb scavenging in the North Atlantic and North Pacific Oceans, *Earth*
774 *and Planetary Science Letters*, *97*(3), 332-352.

775 Cohen, A. S., R. K. O'Nions, R. Siegenthaler, and W. L. Griffin (1988), Chronology of the
776 pressure-temperature history recorded by a granulite terrain, *Contributions to Mineralogy and*
777 *Petrology*, *98*(3), 303-311.

Colin, C., N. Frank, K. Copard, and E. Douville (2010), Neodymium isotopic composition of deep-sea corals from the NE Atlantic: implications for past hydrological changes during the Holocene, *Quaternary Science Reviews*, *29*(19), 2509-2517.

Crocket, K. C., D. Vance, G. L. Foster, D. A. Richards, and M. Tranter (2012), Continental weathering fluxes during the last glacial/interglacial cycle: insights from the marine sedimentary Pb isotope record at Orphan Knoll, NW Atlantic, *Quaternary Science Reviews*, *38*, 89-99.

Crocket, K. C., G. L. Foster, D. Vance, D. A. Richards, and M. Tranter (2013), A Pb isotope tracer of ocean-ice sheet interaction: the record from the NE Atlantic during the Last Glacial/Interglacial cycle, *Quaternary Science Reviews*, *82*, 133-144.

Dausmann, V., M. Gutjahr, M. Frank, K. Kouzmanov, and U. Schaltegger (2019), Experimental evidence for mineral-controlled release of radiogenic Nd, Hf and Pb isotopes from granitic rocks during progressive chemical weathering, *Chemical Geology*, *507*, 64-84.

Diekmann, B., and G. Kuhn (1999), Provenance and dispersal of glacial–marine surface sediments in the Weddell Sea and adjoining areas, Antarctica: ice-rafting versus current transport, *Marine Geology*, *158*(1), 209-231.

Diekmann, B., D. K. Fütterer, H. Grobe, C.-D. Hillenbrand, G. Kuhn, K. Michels, R. Petschick, and M. Pirrung (2003), Ice rafted debris distribution in 16 sediment cores from the South Atlantic, in *Terrigenous sediment supply in the polar to temperate South Atlantic: land-ocean links of environmental changes during the late Quaternary. In: Wefer, G; Mulitza, S & Ratmeyer, V (eds.), The South Atlantic in the Late Quaternary: Reconstruction of Material Budget and Current Systems. Springer-Verlag, Berlin, Heidelberg, New York, 375-399, hdl:10013/epic.15597.d001*, edited.

Du, J., B. A. Haley, and A. C. Mix (2016), Neodymium isotopes in authigenic phases, bottom waters and detrital sediments in the Gulf of Alaska and their implications for paleo-circulation reconstruction, *Geochimica et Cosmochimica Acta*, *193*, 14-35.

Ehrmann, W. U., M. Melles, G. Kuhn, and H. Grobe (1992), Significance of clay mineral assemblages in the Antarctic Ocean, *Marine Geology*, *107*(4), 249-273.

Elmore, A. C., A. M. Piotrowski, J. D. Wright, and A. E. Scrivner (2011), Testing the extraction of past seawater Nd isotopic composition from North Atlantic deep sea sediments and foraminifera, *Geochemistry, Geophysics, Geosystems*, *12*(9).

Erel, Y., J. D. Blum, E. Roueff, and J. Ganor (2004), Lead and strontium isotopes as monitors of experimental granitoid mineral dissolution, *Geochimica et Cosmochimica Acta*, *68*(22), 4649-4663.

Flowerdew, M. J., S. Tyrrell, and V. L. Peck (2013), Inferring sites of subglacial erosion using the Pb isotopic composition of ice-rafted feldspar: Examples from the Weddell Sea, Antarctica, *Geology*, *41*(2), 147-150.

Foster, G. L., and D. Vance (2006), Negligible glacial–interglacial variation in continental chemical weathering rates, *Nature*, *444*(7121), 918-921.

Frank, M. (2002), Radiogenic isotopes: Tracers of past ocean circulation and erosional input, *Reviews of Geophysics*, *40*(1), 1-1-1-38.

Frank, M., and R. K. O'Nions (1998), Sources of Pb for Indian Ocean ferromanganese crusts: a record of Himalayan erosion?, *Earth and Planetary Science Letters*, *158*(3), 121-130.

Frank, M., N. Whiteley, S. Kasten, J. R. Hein, and K. O'Nions (2002), North Atlantic Deep Water export to the Southern Ocean over the past 14 Myr: Evidence from Nd and Pb isotopes in ferromanganese crusts, *Paleoceanography*, *17*(2), 12-11-12-19.

Goldstein, S. L., and S. R. Hemming (2003), 6.17 - Long-lived Isotopic Tracers in Oceanography, Paleoceanography, and Ice-sheet Dynamics, in *Treatise on Geochemistry*, edited by H. D. Holland and K. K. Turekian, pp. 453-489, Pergamon, Oxford.

Gourlan, A. T., L. Meynadier, C. J. Allègre, P. Tapponnier, J.-L. Birck, and J.-L. Joron (2010), Northern Hemisphere climate control of the Bengali rivers discharge during the past 4 Ma, *Quaternary Science Reviews*, *29*(19), 2484-2498.

Gutjahr, M., M. Frank, A. N. Halliday, and L. D. Keigwin (2009), Retreat of the Laurentide ice sheet tracked by the isotopic composition of Pb in western North Atlantic seawater during termination 1, *Earth and Planetary Science Letters*, *286*(3–4), 546-555.

Gutjahr, M., M. Frank, C. H. Stirling, V. Klemm, T. van de Flierdt, and A. N. Halliday (2007), Reliable extraction of a deepwater trace metal isotope signal from Fe–Mn oxyhydroxide coatings of marine sediments, *Chemical Geology*, *242*(3), 351-370.

Haley, B. A., M. Frank, R. F. Spielhagen, and J. Fietzke (2008), Radiogenic isotope record of Arctic Ocean circulation and weathering inputs of the past 15 million years, *Paleoceanography*, *23*(1).

Hathorne, E. C., B. Haley, T. Stichel, P. Grasse, M. Zieringer, and M. Frank (2012), Online preconcentration ICP-MS analysis of rare earth elements in seawater, *Geochemistry, Geophysics, Geosystems*, *13*(1).

Henderson, G. M., and E. Maier-Reimer (2002), Advection and removal of 210Pb and stable Pb isotopes in the oceans: a general circulation model study, *Geochimica et Cosmochimica Acta*, *66*(2), 257-272.

Hillenbrand, C.-D., et al. (2014), Reconstruction of changes in the Weddell Sea sector of the Antarctic Ice Sheet since the Last Glacial Maximum, *Quaternary Science Reviews*, *100*, 111-136.

Howe, J. N. W., A. M. Piotrowski, and V. C. F. Rennie (2016), Abyssal origin for the early Holocene pulse of unradiogenic neodymium isotopes in Atlantic seawater, *Geology*, *44*(10), 831-834.

Huang, H., M. Gutjahr, A. Eisenhauer, and G. Kuhn (2020), No detectable Weddell Sea Antarctic Bottom Water export during the Last and Penultimate Glacial Maximum, *Nature Communications*, *11*(1), 424.

Klevenz, V., D. Vance, D. N. Schmidt, and K. Mezger (2008), Neodymium isotopes in benthic foraminifera: Core-top systematics and a down-core record from the Neogene south Atlantic, *Earth and Planetary Science Letters*, *265*(3), 571-587.

855 Kraft, S., M. Frank, E. C. Hathorne, and S. Weldeab (2013), Assessment of seawater Nd isotope
856 signatures extracted from foraminiferal shells and authigenic phases of Gulf of Guinea sediments,
857 *Geochimica et Cosmochimica Acta*, *121*, 414-435.

858 Kurzweil, F., M. Gutjahr, D. Vance, and L. Keigwin (2010), Authigenic Pb isotopes from the
859 Laurentian Fan: Changes in chemical weathering and patterns of North American freshwater
860 runoff during the last deglaciation, *Earth and Planetary Science Letters*, *299*(3), 458-465.

861 Lacan, F., and C. Jeandel (2005), Neodymium isotopes as a new tool for quantifying exchange
862 fluxes at the continent–ocean interface, *Earth and Planetary Science Letters*, *232*(3), 245-257.

863 Lacan, F., K. Tachikawa, and C. Jeandel (2012), Neodymium isotopic composition of the oceans:
864 A compilation of seawater data, *Chemical Geology*, *300-301*, 177-184.

865 Latimer, J. C., G. M. Filippelli, I. L. Hendy, J. D. Gleason, and J. D. Blum (2006), Glacial-
866 interglacial terrigenous provenance in the southeastern Atlantic Ocean: The importance of deep-
867 water sources and surface currents, *Geology*, *34*(7), 545-548.

868 Lee, J.-M., S. F. Eltgroth, E. A. Boyle, and J. F. Adkins (2017), The transfer of bomb radiocarbon
869 and anthropogenic lead to the deep North Atlantic Ocean observed from a deep sea coral, *Earth*
870 *and Planetary Science Letters*, *458*, 223-232.

871 Lee, J.-M., E. A. Boyle, I. Suci Nurhati, M. Pfeiffer, A. J. Meltzner, and B. Suwargadi (2014),
872 Coral-based history of lead and lead isotopes of the surface Indian Ocean since the mid-20th
873 century, *Earth and Planetary Science Letters*, *398*, 37-47.

874 Lee, J.-M., E. A. Boyle, T. Gamo, H. Obata, K. Norisuye, and Y. Echegoyen (2015), Impact of
875 anthropogenic Pb and ocean circulation on the recent distribution of Pb isotopes in the Indian
876 Ocean, *Geochimica et Cosmochimica Acta*, *170*, 126-144.

877 Lugmair, G. W., and S. J. G. Galer (1992), Age and isotopic relationships among the angrites
878 Lewis Cliff 86010 and Angra dos Reis, *Geochimica et Cosmochimica Acta*, *56*(4), 1673-1694.

879 Martin, E. E., and H. D. Scher (2004), Preservation of seawater Sr and Nd isotopes in fossil fish
880 teeth: bad news and good news, *Earth and Planetary Science Letters*, *220*(1), 25-39.

Martin, E. E., S. W. Blair, G. D. Kamenov, H. D. Scher, E. Bourbon, C. Basak, and D. N. Newkirk (2010), Extraction of Nd isotopes from bulk deep sea sediments for paleoceanographic studies on Cenozoic time scales, *Chemical Geology*, *269*(3), 414-431.

Michels, K., G. Kuhn, C.-D. Hillenbrand, B. Diekmann, D. K. Fütterer, H. Grobe, and G. Uenzelmann-Neben (2002), Grain size composition of sediment cores from the Weddell Sea, Antarctica, in *The southern Weddell Sea: combined contourite-turbidite sedimentation at the southeastern margin of the Weddell Gyre. In: Stow, D A V; Pudsey, C; Howe, J C; Faugères, J-C & Viana, A R (eds.), Deep-water contourite systems: modern drifts and ancient series, seismic and sedimentary characteristics. Geological Society of London, Memoirs, London, 22, 305-323, hdl:10013/epic.14690.d001*, edited, PANGAEA.

Middelburg, J. J., C. H. van der Weijden, and J. R. W. Woittiez (1988), Chemical processes affecting the mobility of major, minor and trace elements during weathering of granitic rocks, *Chemical Geology*, *68*(3), 253-273.

Ndungu, K., C. M. Zurbrick, S. Stammerjohn, S. Severmann, R. M. Sherrell, and A. R. Flegal (2016), Lead Sources to the Amundsen Sea, West Antarctica, *Environmental Science & Technology*, *50*(12), 6233-6239.

Nicholls, K. W., L. Padman, M. Schröder, R. A. Woodgate, A. Jenkins, and S. Østerhus (2003), Water mass modification over the continental shelf north of Ronne Ice Shelf, Antarctica, *Journal of Geophysical Research: Oceans*, *108*(C8).

O'Nions, R. K., M. Frank, F. von Blanckenburg, and H. F. Ling (1998), Secular variation of Nd and Pb isotopes in ferromanganese crusts from the Atlantic, Indian and Pacific Oceans, *Earth and Planetary Science Letters*, *155*(1), 15-28.

Ohr, M., A. N. Halliday, and D. R. Peacor (1991), Sr and Nd isotopic evidence for punctuated clay diagenesis, Texas Gulf Coast, *Earth and Planetary Science Letters*, *105*(1), 110-126.

Orsi, A. H., and T. Whitworth, III (2005), Hydrographic Atlas of the World Ocean Circulation Experiment (WOCE) Volume 1: Southern Ocean.

907 Paul, M., L. Bridgestock, M. Rehkämper, T. van DeFlierdt, and D. Weiss (2015a), High-precision
908 measurements of seawater Pb isotope compositions by double spike thermal ionization mass
909 spectrometry, *Analytica Chimica Acta*, *863*, 59-69.

910 Paul, M., T. van de Flierdt, M. Rehkämper, R. Khondoker, D. Weiss, M. C. Lohan, and W. B.
911 Homoky (2015b), Tracing the Agulhas leakage with lead isotopes, *Geophysical Research Letters*,
912 *42*(20), 8515-8521.

913 Pearce, C. R., M. T. Jones, E. H. Oelkers, C. Pradoux, and C. Jeandel (2013), The effect of
914 particulate dissolution on the neodymium (Nd) isotope and Rare Earth Element (REE) composition
915 of seawater, *Earth and Planetary Science Letters*, *369-370*, 138-147.

916 Planchon, F. A. M., K. van de Velde, K. J. R. Rosman, E. W. Wolff, C. P. Ferrari, and C. F.
917 Boutron (2003), One hundred fifty–year record of lead isotopes in Antarctic snow from Coats Land,
918 *Geochimica et Cosmochimica Acta*, *67*(4), 693-708.

919 Pöppelmeier, F., M. Gutjahr, P. Blaser, L. D. Keigwin, and J. Lippold (2018), Origin of Abyssal
920 NW Atlantic Water Masses Since the Last Glacial Maximum, *Paleoceanography and*
921 *Paleoclimatology*, *33*(5), 530-543.

922 Rempfer, J., T. F. Stocker, F. Joos, J.-C. Dutay, and M. Siddall (2011), Modelling Nd-isotopes
923 with a coarse resolution ocean circulation model: Sensitivities to model parameters and source/sink
924 distributions, *Geochimica et Cosmochimica Acta*, *75*(20), 5927-5950.

925 Reynolds, B. C., M. Frank, and R. K. O'Nions (1999), Nd- and Pb-isotope time series from Atlantic
926 ferromanganese crusts: implications for changes in provenance and paleocirculation over the last
927 8 Myr, *Earth and Planetary Science Letters*, *173*(4), 381-396.

928 Rickli, J., M. Gutjahr, D. Vance, M. Fischer-Gödde, C.-D. Hillenbrand, and G. Kuhn (2014),
929 Neodymium and hafnium boundary contributions to seawater along the West Antarctic continental
930 margin, *Earth and Planetary Science Letters*, *394*, 99-110.

931 Rignot, E., J. Mouginot, and B. Scheuchl (2011), Ice Flow of the Antarctic Ice Sheet, *Science*,
932 *333*(6048), 1427-1430.

933 Rijkenberg, M. J. A., et al. (2015), “PRISTINE”, a new high volume sampler for ultraclean
934 sampling of trace metals and isotopes, *Marine Chemistry*, *177*, 501-509.

935 Roberts, N. L., A. M. Piotrowski, J. F. McManus, and L. D. Keigwin (2010), Synchronous
936 deglacial overturning and water mass source changes, *Science*, *327*(5961), 75-78.

937 Schaule, B. K., and C. C. Patterson (1981), Lead concentrations in the northeast Pacific: evidence
938 for global anthropogenic perturbations, *Earth and Planetary Science Letters*, *54*(1), 97-116.

939 Schlitzer, R., et al. (2018), The GEOTRACES Intermediate Data Product 2017, *Chemical Geology*,
940 *493*, 210-223.

941 Schlosser, C., J. Karstensen, and E. M. S. Woodward (2019), Distribution of dissolved and
942 leachable particulate Pb in the water column along the GEOTRACES section GA10 in the South
943 Atlantic, *Deep Sea Research Part I: Oceanographic Research Papers*.

944 Siddall, M., S. Khatiwala, T. van de Flierdt, K. Jones, S. L. Goldstein, S. Hemming, and R. F.
945 Anderson (2008), Towards explaining the Nd paradox using reversible scavenging in an ocean
946 general circulation model, *Earth and Planetary Science Letters*, *274*(3), 448-461.

947 Staudigel, H., P. Doyle, and A. Zindler (1985), Sr and Nd isotope systematics in fish teeth, *Earth*
948 *and Planetary Science Letters*, *76*(1), 45-56.

949 Stichel, T., M. Frank, J. Rickli, E. C. Hathorne, B. A. Haley, C. Jeandel, and C. Pradoux (2012a),
950 Sources and input mechanisms of hafnium and neodymium in surface waters of the Atlantic sector
951 of the Southern Ocean, *Geochimica et Cosmochimica Acta*, *94*, 22-37.

952 Stichel, T., M. Frank, J. Rickli, and B. A. Haley (2012b), The hafnium and neodymium isotope
953 composition of seawater in the Atlantic sector of the Southern Ocean, *Earth and Planetary Science*
954 *Letters*, *317-318*, 282-294.

955 Strawn, D. G., and D. L. Sparks (2000), Effects of Soil Organic Matter on the Kinetics and
956 Mechanisms of Pb(II) Sorption and Desorption in Soil, *Soil Science Society of America Journal*,
957 *64*(1), 144-156.

Struve, T., T. van de Flierdt, A. Burke, L. F. Robinson, S. J. Hammond, K. C. Crocket, L. I. Bradtmiller, M. E. Auro, K. J. Mohamed, and N. J. White (2017), Neodymium isotopes and concentrations in aragonitic scleractinian cold-water coral skeletons - Modern calibration and evaluation of palaeo-applications, *Chemical Geology*, *453*, 146-168.

Süfke, F., M. Gutjahr, A. Gilli, F. S. Anselmetti, L. Glur, and A. Eisenhauer (2019), Early stage weathering systematics of Pb and Nd isotopes derived from a high-Alpine Holocene lake sediment record, *Chemical Geology*, *507*, 42-53.

Tachikawa, K., C. Jeandel, and M. Roy-Barman (1999), A new approach to the Nd residence time in the ocean: the role of atmospheric inputs, *Earth and Planetary Science Letters*, *170*(4), 433-446.

Tachikawa, K., V. Athias, and C. Jeandel (2003), Neodymium budget in the modern ocean and paleo-oceanographic implications, *Journal of Geophysical Research: Oceans*, *108*(C8).

Tanaka, T., et al. (2000), JNdi-1: a neodymium isotopic reference in consistency with LaJolla neodymium, *Chemical Geology*, *168*(3), 279-281.

Tessier, A., P. G. C. Campbell, and M. Bisson (1979), Sequential extraction procedure for the speciation of particulate trace metals, *Analytical Chemistry*, *51*(7), 844-851.

Thirlwall, M. F. (2002), Multicollector ICP-MS analysis of Pb isotopes using a 207Pb-204Pb double spike demonstrates up to 400 ppm/amu systematic errors in Tl-normalization, *Chemical Geology*, *184*(3), 255-279.

van de Flierdt, T., L. F. Robinson, J. F. Adkins, S. R. Hemming, and S. L. Goldstein (2006), Temporal stability of the neodymium isotope signature of the Holocene to glacial North Atlantic, *Paleoceanography*, *21*(4).

van de Flierdt, T., M. Frank, A. N. Halliday, J. R. Hein, B. Hattendorf, D. Günther, and P. W. Kubik (2004), Deep and bottom water export from the Southern Ocean to the Pacific over the past 38 million years, *Paleoceanography*, *19*(1).

Vance, D., and K. Burton (1999), Neodymium isotopes in planktonic foraminifera: a record of the response of continental weathering and ocean circulation rates to climate change, *Earth and Planetary Science Letters*, *173*(4), 365-379.

Vance, D., and M. Thirlwall (2002), An assessment of mass discrimination in MC-ICPMS using Nd isotopes, *Chemical Geology*, *185* (3-4), 227-240.

Vernet, M., et al. (2019), The Weddell Gyre, Southern Ocean: Present Knowledge and Future Challenges, *Reviews of Geophysics*, *57*(3), 623-708.

Wilson, D. J., T. van de Flierdt, and J. F. Adkins (2017), Lead isotopes in deep-sea coral skeletons: Ground-truthing and a first deglacial Southern Ocean record, *Geochimica et Cosmochimica Acta*, *204*, 350-374.

Wilson, D. J., A. M. Piotrowski, A. Galy, and J. A. Clegg (2013), Reactivity of neodymium carriers in deep sea sediments: Implications for boundary exchange and paleoceanography, *Geochimica et Cosmochimica Acta*, *109*, 197-221.

Wilson, D. J., K. C. Crocket, T. van de Flierdt, L. F. Robinson, and J. F. Adkins (2014), Dynamic intermediate ocean circulation in the North Atlantic during Heinrich Stadial 1: A radiocarbon and neodymium isotope perspective, *Paleoceanography*, *29*(11), 1072-1093.

Wu, J., R. Rember, M. Jin, E. A. Boyle, and A. R. Flegal (2010), Isotopic evidence for the source of lead in the North Pacific abyssal water, *Geochimica et Cosmochimica Acta*, *74*(16), 4629-4638.

Yusoff, Z. M., B. T. Ngwenya, and I. Parsons (2013), Mobility and fractionation of REEs during deep weathering of geochemically contrasting granites in a tropical setting, Malaysia, *Chemical Geology*, *349-350*, 71-86.

Zweng, M. M., et al. (2013), Salinity, *World Ocean Atlas 2013.*, *2*.